

# A self-consistent spectral framework for inclusive non-elastic breakup, with the Trojan Horse method as the sub-Coulomb resonant limit

Jin Lei\*

*School of Physics Science and Engineering, Tongji University, Shanghai 200092, China. and  
Southern Center for Nuclear-Science Theory (SCNT), Institute of Modern Physics,  
Chinese Academy of Sciences, Huizhou 516000, Guangdong Province, China.*

(Dated: May 19, 2026)

The Trojan Horse Method (THM) extracts low-energy charged-particle resonance strengths through a plane-wave impulse approximation (PWIA) reduction of a three-body transfer matrix element. The Ichimura-Austern-Vincent (IAV) inclusive non-elastic breakup framework has been widely applied at intermediate and high energies but has not been brought to the sub-Coulomb astrophysical regime where THM operates; the validity of the PWIA reduction there has accordingly not been assessed in a controlled framework that links the IAV inclusive cross section to the underlying per-pole distorted-wave Born approximation (DWBA) pole amplitude. I introduce a diagonal isolated-pole spectral ansatz for the absorptive participant-target optical potential, formulated through three validity conditions; two of these reduce to closed dimensionless bounds in terms of widths and level spacings computable from  $R$ -matrix tabulations, while the third, decoupling from the genuine  $x+A$  continuum, is a model-dependent diagnostic closed once a continuum model is specified. Within this ansatz the IAV inclusive non-elastic breakup cross section reduces in the isolated-resonance limit to a sum of per-pole DWBA pole cross sections weighted by channel branching ratios; a three-layer Feshbach decomposition gives the width dictionary  $\xi_n^{\text{IAV}} = \Gamma_n^{\text{non-el}}/2 \simeq \Gamma_n^{\text{tot}}/2$ , resolving half-width-versus-full-width and sign ambiguities in the literature and the conflation of the spectral pole half-width with the participant-channel partial width. The factorized PWIA-THM resonance-strength formula is then identified as a non-perturbative reduction of the per-pole DWBA cross section under four approximations: plane-wave substitution on the entrance and exit distorted waves, zero-range or surface-localized treatment of the spectator-participant interaction, on-shell evaluation of the binary subreaction vertex, and post-form remnant neglect. The per-pole DWBA pole cross section, not a multiplicative correction factor on top of PWIA-THM, is identified as the natural extraction quantity for sub-Coulomb resonance-strength analysis within this spectral framework.

## I. INTRODUCTION

The Trojan Horse Method (THM) is a principal indirect method for measuring resonance strengths of low-energy charged-particle reactions at energies relevant to stellar nucleosynthesis, where the entrance channel is suppressed by the Coulomb barrier of the binary subreaction [1–5]. The method extracts the resonance strength of a binary subreaction  $A(x, c)B$  at sub-Coulomb energies from a quasi-free three-body breakup  $A(a, cb)B$  with  $a = b + x$ , in which the Trojan Horse particle  $a$  delivers the participant  $x$  to the target  $A$  above the Coulomb barrier of the projectile  $a$  while the spectator  $b$  carries away the excess kinetic energy, so that the  $x + A$  binary subreaction occurs at sub-Coulomb relative energy. The working extraction formula in current use throughout the indirect-method community is a plane-wave impulse approximation (PWIA) reduction of an underlying transfer matrix element [6–11]. In this reduction the entrance distorted wave of the Trojan Horse particle relative to the target and the exit distorted wave of the spectator relative to the residual are both replaced by plane waves, the spectator-participant relative motion inside the Trojan Horse is represented by the Fourier transform of its

internal wavefunction, and the binary subreaction cross section is read from the remaining factorized expression.

The PWIA reduction is operationally performed at the quasi-free (QF) kinematic condition characteristic of THM measurements: spectator-detection cuts select configurations at the peak of the bound-state momentum amplitude  $|\tilde{\phi}_a(\mathbf{p}_{bx})|^2$ , where  $\tilde{\phi}_a$  is the Fourier transform of the Trojan Horse internal wavefunction  $\phi_a$  with respect to the spectator-participant relative coordinate; for the s-wave-dominated Trojan Horses in standard use (deuteron,  $^3\text{He}$ ,  $^6\text{Li}$ ) the peak lies at  $\mathbf{p}_{bx} \approx 0$ . The factorized expression contains a half-off-energy-shell (HOES) binary amplitude at the corresponding effective relative energy whose connection to the on-shell binary cross section is treated as a separate extrapolation step in the THM literature. The QF condition is the standard kinematic context of all current PWIA-THM extractions and is taken as given throughout the present analysis; what is at issue is not the QF kinematic selection itself but the dynamical content of the PWIA reduction performed at the QF kinematic point.

The validity of the PWIA reduction at sub-Coulomb energies has been raised by several groups but not assessed in a controlled framework. The earliest controlled treatment of off-energy-shell corrections in the THM context, by Tumino, Mukhamedzhanov, and collaborators [12], was restricted to elastic two-body subreactions and

\* jinl@tongji.edu.cn

to s-wave separable Yamaguchi potentials. A later line of work by Mukhamedzhanov, Kadyrov, and collaborators [13–15] extended the off-energy-shell treatment of the binary vertex through a generalized  $R$ -matrix and surface-integral approach. Both treatments capture the off-shell extrapolation of the binary subreaction vertex but do not include the entrance and exit distortions of the three-body process, nor the post-form remnant that arises when the participant-target interaction is non-Hermitian. Bertulani, Hussein, and Typel [16] explicitly labeled the inclusive-to-PWIA reduction of the indirect cross section as a chain of approximations awaiting assessment. The recent comprehensive review of the THM by Tumino *et al.* [17] summarizes the modified-DWBA framework that incorporates the entrance and exit distortions, and presents the resonant case as a sum of isolated non-interfering one-level two-channel  $R$ -matrix half-off-shell amplitudes. Its Ichimura-Austern-Vincent non-elastic-breakup (IAV-NEB) discussion presents this cross section in closed form but does not project this parent inclusive expression onto its narrow-resonance limit as a sum of Lorentzian-weighted per-pole transfer cross sections, nor does it document the systematic non-perturbative reduction chain from the per-pole DWBA pole amplitude to the factorized PWIA-THM extraction. A controlled link from the parent inclusive cross section to the per-pole DWBA pole amplitude that underlies the factorized PWIA-THM working formula, with the four-step approximation chain (plane-wave substitution, zero-range or surface-localized  $V_{bx}$ , on-shell binary vertex, post-form remnant neglect) made explicit, has not appeared in the published THM literature.

The quantitative stakes of the validity question have grown sharply through the case of the  $^{19}\text{F}(p, \alpha\gamma)^{16}\text{O}$  reaction, whose rate has been repeatedly revisited through compilations, direct measurements, indirect measurements, and  $R$ -matrix analyses [2, 5, 9, 10, 18–21]. In this case a recent THM measurement of the 11 keV resonance strength [11] disagrees, by approximately a factor of six in the partial decay strength, with the  $R$ -matrix evaluation of the same  $^{19}\text{F}(p, \alpha\gamma)^{16}\text{O}$  channel that uses JUNA direct measurements above  $\approx 70$  keV and partner-channel  $^{19}\text{F}(p, \gamma)^{20}\text{Ne}$  measurements as anchors and propagates them to the 11 keV near-threshold pole through a global  $R$ -matrix fit with previously tabulated proton-channel input [22–26]. The consequences propagate into Population III calcium production estimates [20, 24]. The disagreement is a prominent current quantitative tension in low-energy nuclear astrophysics, and concentrates the validity question of the PWIA reduction into a quantitative target. The framework constructed in the present manuscript is general for any sub-Coulomb resonant THM benchmark in the narrow-resonance regime.

The IAV framework supplies the inclusive non-elastic-breakup cross section of any three-body breakup with a complex participant-target optical potential [27–29]. The original derivation of Ref. [27] gives the inclusive

cross section as a Green-function expectation value of the imaginary part of the participant-target potential. A recent line of work has revisited the IAV framework with controlled post-prior equivalence [30–32], with an angular-momentum-basis extension to arbitrary partial waves [33], and with continuum-discretized coupled-channel wavefunctions through numerical benchmarks [34] and a formal post-form derivation [35]. Among these, Ref. [32], in particular, derives a Breit-Wigner spectral decomposition of the IAV cross section in the form of a sum over narrow poles of the participant-target Green function  $G_x(E_x) = (E_x - T_x - U_x)^{-1}$ , each pole located at  $E_x = E_n - i\xi_n^{\text{IAV}}$  in the lower complex-energy half-plane and identified one-to-one with a narrow resonance state  $\phi_n$  in the energy window of interest; in its narrow-resonance limit the inclusive cross section reduces to a Lorentzian-weighted single-pole transfer matrix element evaluated at the resonance energy. This narrow-resonance projection is the natural starting point for sub-Coulomb resonant THM extraction. A direct application of the projection to a THM benchmark has not appeared in the published literature.

Two related lines of work raise the question of whether a numerical implementation of the IAV-to-THM intersection is feasible. Mukhamedzhanov, Pang, and Kadyrov [36] formulate the THM cross section through a surface-integral and off-shell decomposition that includes a vertex form factor, an off-shell function, and a Coulomb Jost function. The numerical implementation of that paper, however, evaluates only a renormalization factor built from the ratio of zero-range DWBA cross sections weighted by the spectator momentum distribution, in which the off-shell function, Coulomb Jost, and vertex form factor of their analytical framework cancel or are absent; the full surface-integral expression is not the object evaluated in the production calculation. Their conclusion that the inclusion of distorted waves eliminates a sharp rise of the indirect S-factor at sub-Coulomb energies is therefore obtained from the zero-range DWBA ratio rather than from the full inclusive parent. The IAV-revival groups [37–40] implement the IAV inclusive non-elastic breakup formalism in different production codes, applied to inclusive breakup at intermediate and high energies; none of these implementations targets a sub-Coulomb THM benchmark or evaluates the narrow-resonance projection of the inclusive parent.

The aim of the present work is to build the analytical framework that connects the parent IAV inclusive cross section to the THM extraction at sub-Coulomb energies through a diagonal isolated-pole spectral ansatz on the absorptive part of the participant-target optical potential, formulated with three explicit validity conditions of which two reduce to closed dimensionless bounds from  $R$ -matrix tabulations and the third is a model-dependent continuum-decoupling diagnostic. I establish a width dictionary  $\xi_n^{\text{IAV}} = \Gamma_n^{\text{non-el}}/2 \simeq \Gamma_n^{\text{tot}}/2$  through a three-layer Feshbach decomposition that resolves the half-width versus full-width and sign-of-the-imaginary-

potential ambiguities of the literature and the recurring conflation of the spectral pole half-width with the participant-channel partial width, and adopt a controlled post-form source convention for the transfer matrix element at sub-Coulomb energies. Within the ansatz, the inclusive non-elastic breakup cross section of the IAV framework reduces under the isolated-resonance limit to a single-pole Breit-Wigner contribution that recovers the THM resonance-strength extraction with an explicit account of the partial-wave coherence and the post-form remnant content of the transfer matrix element.

The overlapping-resonance regime of the same spectral form, in which  $\xi_n^{\text{IAV}} \gtrsim |E_n - E_m|$  and the diagonal ansatz no longer applies, would reorganize formally under three additional averaging assumptions (energy averaging on a window encompassing many resonances, random phases of the off-diagonal couplings, and the local-density approximation) into a Hauser-Feshbach cross section and would recover, in that regime, the surrogate-method picture of compound-nucleus indirect measurement [37–39, 41]; a controlled derivation of that limit is outside the scope of the present work and is left as outlook.

The framework also exposes the dynamical content of the transfer matrix element that the plane-wave reduction suppresses, namely the partial-wave coherence within each pole amplitude and the post-form remnant carried by the difference of the spectator-target and spectator-residual optical potentials. I expose the standard factorized PWIA-THM resonance-strength expression as a non-perturbative reduction of the per-pole distorted-wave Born approximation pole cross section under four identifiable approximations (plane-wave substitution on the entrance and exit distorted waves, zero-range or surface-localized treatment of the spectator-participant interaction, on-shell evaluation of the binary subreaction vertex, and post-form remnant neglect), and I identify the partial-wave coherence and the post-form remnant content as the dynamical content of the transfer matrix element that the reduction discards. The pure plane-wave Born substitution and the further THM factorization approximations are kept separate, so that the partial-wave coherence and the post-form remnant content are identifiable contributions rather than part of an undefined “distortion correction”. No multiplicative dynamical correction factor on top of the PWIA-THM expression is introduced; the operational quantity for sub-Coulomb resonance-strength extraction is the per-pole DWBA pole cross section itself.

The remainder of the paper is organized as follows. Section II recapitulates the IAV inclusive non-elastic breakup framework and its Breit-Wigner spectral form. Section III introduces the diagonal isolated-pole spectral ansatz of the absorptive optical potential and states its three validity conditions. Section IV derives the width dictionary and the integrated-pole-area formulation of the inclusive cross section, including the channel-projection from the inclusive yield to the experimental

exclusive channel. Section V adopts the post-form source as the controlled central convention, identifies the sub-Coulomb obstacle to a per-pole prior-form reduction with a smooth global participant-target real potential, and gives the operator-side post-form remnant decomposition of the per-pole transfer matrix element. Section VI establishes the isolated-resonance limit of the spectral form, in which the Lorentzian profile collapses to a Dirac delta on the resonance energy and the spectral sum recovers the THM extraction; the overlapping-resonance regime is discussed there only as outlook. Section VII relates the present framework to the IAV-revival numerical literature and to the surface-integral formulation of Ref. [36]. Section VIII summarizes the analytical results.

## II. IAV INCLUSIVE NON-ELASTIC BREAKUP AND ITS BREIT-WIGNER SPECTRAL FORM

I consider an inclusive non-elastic breakup reaction of the form  $a + A \rightarrow b + B^*$ , where the projectile  $a = b + x$  separates into a detected spectator  $b$  and an unobserved residual system  $B^*$  that denotes any (bound, resonant, or continuum) non-elastic final state of the  $x + A$  composite. The participant  $x$  undergoes a non-elastic interaction with the target  $A$ , and only the spectator  $b$  is observed. The inclusive non-elastic breakup cross section, summed over all final states of the  $x + A$  subsystem except the elastic  $x + A$  channel, was derived in Ref. [27] in post form and reads

$$\frac{d^2\sigma_{\text{NEB}}}{d\Omega_b dE_b} = -\frac{2}{\hbar v_a} \rho_b(E_b) \langle \psi_x(\mathbf{k}_b) | W_x | \psi_x(\mathbf{k}_b) \rangle, \quad (1)$$

where  $v_a = \hbar k_a / \mu_a$  is the projectile velocity in the entrance channel with relative momentum  $k_a$  and reduced mass  $\mu_a$ ,  $\rho_b(E_b) = \mu_b k_b / [(2\pi)^3 \hbar^2]$  is the spectator phase-space density at spectator relative momentum  $k_b$  and reduced mass  $\mu_b$  in the exit channel,  $W_x = \text{Im} U_x$  is the imaginary part of the complex participant-target optical potential, and  $\psi_x(\mathbf{k}_b, \mathbf{r}_x)$  is the participant spectator wavefunction defined as the solution of an inhomogeneous Schrödinger equation with complex participant-target optical potential  $U_x$  and outgoing-wave boundary conditions, with the source set by the post-form interaction [27, 31, 32]. The asymptotic outgoing-wave amplitude of  $\psi_x$  in the  $x + A$  elastic channel carries the elastic-breakup (EBU) content of the three-body process, in which  $A$  remains in its ground state, while the matrix element  $\langle \psi_x(\mathbf{k}_b) | W_x | \psi_x(\mathbf{k}_b) \rangle$  projects out the flux removed from this elastic channel into the non-elastic decay channels, so that Eq. (1) counts only the non-elastic breakup yield. I adopt the post-form throughout this manuscript; Eq. (1) is the canonical post-form inclusive cross section and is the starting point of the present analysis.

The participant-target propagation enters Eq. (1) through the factor  $\langle \psi_x(\mathbf{k}_b) | W_x | \psi_x(\mathbf{k}_b) \rangle$ , which is the expectation value of the absorptive part of the optical po-

tential evaluated on the participant spectator wavefunction. This factor encodes the entire dependence of the inclusive cross section on the dynamics of the  $x + A$  subsystem and is the operational quantity to be approximated when one descends from the inclusive parent toward an extraction formula for an individual resonance.

In the narrow-resonance regime the spectral structure of the participant-target propagator is dominated by a discrete set of isolated resonance states  $\{\phi_n\}$  in the energy window of interest. The symbol  $\phi_n$  is used throughout this manuscript for the single-particle resonance form factor in the standard Lane-Thomas  $R$ -matrix interior convention [3, 42]: the interior eigenfunction of  $(T_x + V_x^R)\phi_n = E_n\phi_n$  on the region  $r \leq a$  with the Bloch boundary operator imposed at  $r = a$ , where  $V_x^R$  is a real participant-target potential adjusted so that the eigenvalue equals the experimental resonance energy  $E_n$ , and  $u_l(r) = r\phi_n(r)$  is normalized to unit probability over  $r \leq a$ . The form factors  $\{\phi_n\}$  are therefore not  $L^2$  eigenstates of the full participant-target Hamiltonian above the  $x + A$  threshold, and they are not mutually orthogonal in the  $L^2$  sense across the channel surface; they are interior-normalized form factors on which the per-pole DWBA transfer matrix element acts. The asymptotic Coulomb tail of  $\phi_n$  beyond  $r = a$  is not constructed explicitly; it is encoded in the surface amplitude  $u_l(a)$ , through which the standard  $R$ -matrix surface relation (12) of Sec. IV fixes the partial widths. The spectral expansion of the absorptive operator  $W_x$  on this form-factor basis, introduced in Eq. (5) of Sec. III below, is therefore an effective rank- $N$  projection on the resonance form factors of the energy window of interest rather than a literal Hilbert-space resolution of identity. The complement of this projection consists of the smooth non-resonant  $x + A$  scattering states of the participant-target subsystem; the requirement that  $W_x$  carries negligible absorption on these states is stated below as condition (A2) of the spectral ansatz. Inserting the resulting spectral expansion of the propagator into Eq. (1) and reorganizing, Lei and Moro [32] derived the spectral form rigorously for constant  $W_x$ . The same algebraic step extends without modification to diagonal  $W_x$  on the resonance-state basis  $\{\phi_n\}$ , with perturbative corrections from the off-diagonal couplings of  $W_x$  in the general case; the diagonality is promoted to a controlled ansatz with explicit validity conditions in Sec. III. The spectral form reads

$$\frac{d^2\sigma_{\text{NEB}}}{d\Omega_b dE_b} = \sum_n \omega_n(E_x) \frac{d\sigma_n^{\text{DWBA}}}{d\Omega_b}, \quad (2)$$

where  $E_x$  is the participant-target subsystem energy reconstructed from the measured spectator energy  $E_b$ , and the spectral weight  $\omega_n(E_x)$  is the Lorentzian profile

$$\omega_n(E_x) = \frac{\xi_n^{\text{IAV}}/\pi}{(E_x - E_n)^2 + (\xi_n^{\text{IAV}})^2}, \quad (3)$$

peaked at  $E_x = E_n$  with full width at half maximum  $2\xi_n^{\text{IAV}}$ . The pole transfer cross section appearing in

Eq. (2) is the standard distorted-wave Born approximation transfer matrix element evaluated on the resonance state  $\phi_n$ ,

$$\begin{aligned} \frac{d\sigma_n^{\text{DWBA}}}{d\Omega_b} &= \frac{2\pi \rho_b}{\hbar v_a} |\mathcal{M}_n^{\text{DWBA}}|^2, \\ \mathcal{M}_n^{\text{DWBA}} &\equiv \langle \phi_n \chi_b^{(-)} | V_{\text{post}} | \chi_a^{(+)} \phi_a \rangle, \end{aligned} \quad (4)$$

in which  $\chi_a^{(+)}(\mathbf{k}_a, \mathbf{r}_a)$  is the entrance distorted wave generated by the projectile-target optical potential,  $\chi_b^{(-)}(\mathbf{k}_b, \mathbf{r}_b)$  is the exit distorted wave generated by the spectator-residual optical potential,  $\phi_a$  is the projectile internal wavefunction in the bound configuration  $a = b + x$ , and  $V_{\text{post}} = V_{bx} + (U_{bA} - U_{bB})$  is the post-form interaction (here  $V_{bx}$  is the spectator-participant interaction inside the projectile,  $U_{bA}$  is the spectator-target optical potential, and  $U_{bB}$  is the spectator-residual optical potential). The matrix element  $\mathcal{M}_n^{\text{DWBA}}$  of Eq. (4) decomposes in the Lane-Thomas  $R$ -matrix interior convention [3, 42] into a volume integral over the interior region  $r_x \leq a$  (where  $\phi_n$  is supported by the unit-interior normalization of  $u_l = r\phi_n$ ) plus a surface contribution at  $r_x = a$  from the Bloch boundary operator. The surface contribution captures, via the surface term from integrating  $T_x$  by parts on  $r \leq a$ , the participant-channel asymptotic content of the matrix element that is not built into  $\phi_n$  on  $r > a$ ; volume and surface together define  $\mathcal{M}_n^{\text{DWBA}}$  unambiguously in this convention. All per-pole DWBA cross sections in this manuscript are understood as magnetic-substate-summed in the exit channel and entrance-channel-spin-averaged over the projectile-target  $(2j_a + 1)(2j_A + 1)$  entrance substates of the three-body process; the binary resonance statistical factor  $(2J_n + 1)/[(2j_x + 1)(2j_A + 1)]$  that enters the astrophysical resonance strength of Eq. (24) below is a distinct object that appears when projecting the per-pole DWBA cross section onto the binary  $x + A \rightarrow n$  subreaction. The explicit spin-projection structure is suppressed in Eq. (4) for notational economy and is reinstated whenever a quantitative resonance-strength comparison is made. The detailed properties of  $V_{\text{post}}$ , and the physical reason why the prior-form alternative is not under controlled approximation in the sub-Coulomb regime, are deferred to Sec. V.

A resonance  $n$  can decay through several open channels, including elastic  $x + A$  re-emission with participant-channel partial width  $\Gamma_x^n$ , and the non-elastic decay channels (e.g.  $\alpha$  and  $\gamma$  for the  $^{19}\text{F} + p$  resonances of immediate interest) with partial widths  $\Gamma_c^n$  for  $c \neq x$ , and total width  $\Gamma_n^{\text{tot}} = \Gamma_x^n + \Gamma_n^{\text{non-el}}$  where  $\Gamma_n^{\text{non-el}} = \sum_{c \neq x} \Gamma_c^n$ . The absorptive operator  $W_x$  removes flux from the elastic channel into the non-elastic decay manifold of the resonance; the half-width  $\xi_n^{\text{IAV}}$  of Eq. (3) is therefore the diagonal matrix element of  $W_x$  on  $\phi_n$ ,  $\xi_n^{\text{IAV}} = |\langle \phi_n | W_x | \phi_n \rangle|$ . Its further identification with the sum of non-elastic partial widths,  $\xi_n^{\text{IAV}} = \Gamma_n^{\text{non-el}}/2$ , is the Lane-Thomas  $R$ -matrix result derived in Sec. IV.

Equations (2)-(4) are the canonical Breit-Wigner spec-

tral decomposition of the IAV inclusive non-elastic breakup cross section in the narrow-resonance regime. They identify, on a per-resonance basis, the dynamical content of the inclusive cross section: a Lorentzian energy profile  $\omega_n$  that is set by the participant-target propagator alone, and a coherent partial-wave transfer matrix element that is set by the entrance and exit distortions and by the resonance state  $\phi_n$ . The PWIA-THM extraction formula in current use is obtained from Eqs. (2)-(4) by a chain of finite, non-perturbative approximations on the per-pole transfer matrix element of Eq. (4), namely replacing  $\chi_a^{(+)}$  and  $\chi_b^{(-)}$  by plane waves, applying a zero-range or surface-localized treatment to the spectator-participant interaction  $V_{bx}$ , evaluating the binary subreaction vertex on-shell, and dropping the post-form remnant, as explicitly enumerated in Sec. V. The structure of the spectral decomposition exposes that the dynamical content discarded in this reduction chain is encoded in the partial-wave coherence of the transfer matrix element of Eq. (4) and in the post-form interaction  $V_{\text{post}}$ .

### III. DIAGONAL ISOLATED-POLE SPECTRAL ANSATZ OF THE ABSORPTIVE OPTICAL POTENTIAL

The spectral form (2) is exact only when the absorptive participant-target potential acts diagonally on the chosen resonance-state pole basis and is decoupled from the genuine continuum of the participant-target subsystem. In the sub-Coulomb astrophysical regime the absorptive potential is not smooth on the resonance scale: it is dominated by sparse narrow resonances of the participant-target subsystem rather than by the smooth megaelectronvolt-scale optical average that justifies smooth- $W_x$  optical models at higher energies. I therefore introduce the spectral form as an explicit ansatz with three validity conditions that I make testable rather than assume. The role of this ansatz as the first of two non-perturbative reductions from the parent inclusive cross section to the factorized PWIA-THM extraction is summarized in Fig. 1.

The ansatz is the diagonal isolated-pole representation of the absorptive kernel restricted to the pole subspace,

$$W_x \simeq \sum_n |\phi_n\rangle W_n \langle\phi_n|, \quad (5)$$

in which  $\{\phi_n\}$  is the set of isolated resonance states of the participant-target subsystem in the energy window of interest and  $W_n = \langle\phi_n|W_x|\phi_n\rangle$  is the diagonal absorptive matrix element on the corresponding pole form factor. The matrix element  $W_n$  encodes the absorption of the resonance state into the non-elastic decay channels, that is, into the complement of the elastic  $x + A$  channel that  $W_x$  removes flux from; its identification with the non-elastic decay-width sum  $\Gamma_n^{\text{non-el}}/2$  (which collapses to the experimental total decay width  $\Gamma_n^{\text{tot}}/2$  in the sub-Coulomb limit where the participant-channel

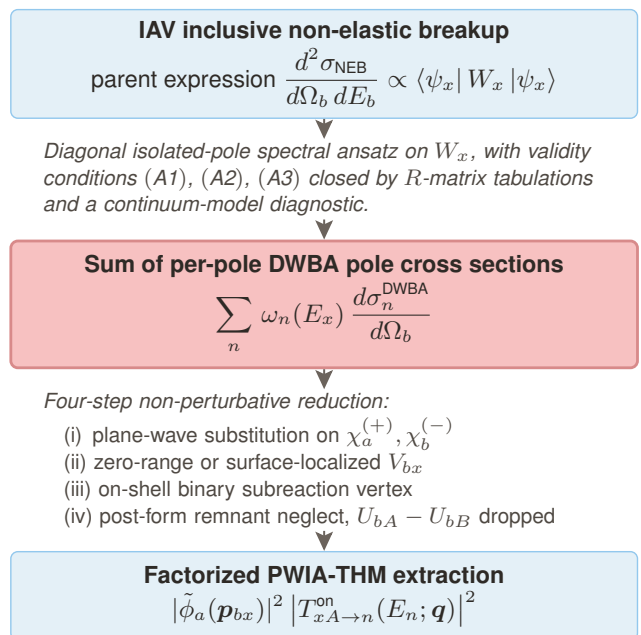


FIG. 1. Two-step non-perturbative reduction from the IAV inclusive non-elastic breakup parent [Eq. (1)] to the factorized PWIA-THM formula [Eq. (18)] of the THM literature [3, 6, 11]. The per-pole DWBA pole cross section at the intermediate level (highlighted) is the operational extraction quantity for sub-Coulomb resonance-strength analysis; the factorized PWIA-THM expression is a downstream non-perturbative reduction of the same parent, not a multiplicative correction factor. More details on the spectral ansatz and validity conditions (A1), (A2), (A3) in Sec. III, and on the four-step reduction in Sec. V.

partial width  $\Gamma_x^n \ll \Gamma_n^{\text{non-el}}$ ) that sets the Lorentzian denominator of the inclusive yield is established as a separate identification in Sec. IV, through a three-layer Feshbach decomposition that distinguishes the role of  $W_x$  on the participant-target propagator, the role of the channel projection that decomposes the non-elastic absorption into specific exit channels, and the role of the participant-channel entrance reduced width that controls the formation amplitude. Equation (5) is therefore not a global spectral representation of the optical potential at all energies; it is the diagonal pole truncation of the absorptive operator  $W_x$  within the resonance subspace spanned by  $\{|\phi_n\rangle\}$  in the narrow energy interval where the isolated resonances dominate. Consistent with the interior-normalized, non-mutually-orthogonal nature of  $\{\phi_n\}$  noted in Sec. II, the ket-bra form of Eq. (5) is to be read as an effective rank- $N$  projection on the resonance form factors rather than as a literal Hilbert-space resolution of identity; the off-diagonal corrections that the form-factor non-orthogonality across  $r = a$  would induce are bounded by condition (A1) and the Cauchy-Schwarz inequality (6) derived below. The ansatz is exact when the following three conditions hold:

- (A1) **Diagonality of  $W_x$  on the pole basis.** The off-diagonal matrix elements  $W_{nm} = \langle \phi_n | W_x | \phi_m \rangle$  for  $n \neq m$  vanish.
- (A2) **Continuum decoupling.** In addition to the resonance states  $\{\phi_n\}$ , the participant-target subsystem has a smooth, non-resonant continuum of  $x+A$  scattering states  $\{\phi_E\}$  that fills the energy gaps between the resonances. Condition (A2) asserts that  $W_x$  has no significant matrix elements involving these non-resonant states: all matrix elements of  $W_x$  that touch a  $\phi_E$  on either side,  $\langle \phi_n | W_x | \phi_E \rangle$  or  $\langle \phi_E | W_x | \phi_{E'} \rangle$ , are negligible against the diagonal pole elements  $W_n = \langle \phi_n | W_x | \phi_n \rangle$ . Physically, the absorption represented by  $W_x$  flows entirely through the discrete resonances and not through the smooth non-resonant  $x+A$  scattering, so the rank- $N$  pole expansion (5) does not miss any absorptive strength.
- (A3) **Pole isolation.** Each resonance  $n$  has a half-width  $\xi_n^{\text{IAV}} = |W_n|$  (identified with  $\Gamma_n^{\text{non-el}}/2 \simeq \Gamma_n^{\text{tot}}/2$  through the three-layer Feshbach decomposition of Sec. IV, with the second equality the sub-Coulomb approximation  $\Gamma_x^n \ll \Gamma_n^{\text{non-el}}$ ) small against the spacing to the nearest neighbor.

Conditions (A1) and (A3) are treated as controlled approximations under explicit dimensionless analytical bounds derived in this section from  $R$ -matrix tabulations; condition (A2) is treated as a model-dependent diagnostic that closes once a continuum model is specified, by the construction developed below.

I treat  $W_x$  as a scalar (central) absorptive potential throughout. Phenomenological global nucleon optical-model parametrizations [43] are fitted in an averaged-resonance regime that is precisely the regime the spectral ansatz (5) is built to resolve (see Sec. V), so they cannot themselves be invoked as evidence for the dominance of the central part on the individual narrow resonances; non-central components such as imaginary spin-orbit are kept out as a working assumption. With the absorptive convention  $W_x \leq 0$  adopted throughout this manuscript (so that  $-W_x$  is a positive-semidefinite quadratic form, Sec. IV), the off-diagonal couplings  $W_{nm}$  vanish for unequal spin-parity by rotational invariance, and for equal spin-parity satisfy the Cauchy-Schwarz bound

$$\begin{aligned} |W_{nm}|^2 &\leq \langle \phi_n | (-W_x) | \phi_n \rangle \langle \phi_m | (-W_x) | \phi_m \rangle \\ &= \xi_n^{\text{IAV}} \xi_m^{\text{IAV}}. \end{aligned} \quad (6)$$

The diagonal-ansatz controlling ratio is therefore

$$\frac{|W_{nm}|}{|E_n - E_m|} \leq \frac{\sqrt{\xi_n^{\text{IAV}} \xi_m^{\text{IAV}}}}{|E_n - E_m|}, \quad (7)$$

small whenever the participant-target subsystem is in the narrow-resonance regime; the explicit evaluation at any specific anchor requires only the experimental partial widths and level energies of the participant-target subsystem.

The validity of (A2) is the requirement that  $W_x$  have negligible matrix elements between the resonance form factors  $\{\phi_n\}$  and the smooth non-resonant  $x+A$  continuum. The split here is one of representation: a resonance is itself a pole of the full  $x+A$  scattering amplitude, and the spectral ansatz separates the spectrum into interior pole form factors on which  $W_x$  is allowed to act and a smooth non-resonant complement on which (A2) requires its absorptive matrix elements to be small. The continuum contribution to the absorptive strength is diagnosed, in a specified continuum model, by the dimensionless ratio

$$\epsilon_{(A2)} \equiv \frac{\sigma_R^{\text{cont}}(\Delta E)}{\sigma_R^{\text{res}}(\Delta E)}, \quad (8)$$

where  $\sigma_R^{\text{res}}(\Delta E)$  is the contribution to the total  $x+A$  reaction cross section integrated over the energy window  $\Delta E$  of interest from the resonance-pole sector  $\{\phi_n\}$  (the sum of narrow-resonance pole terms in an  $R$ -matrix decomposition, or the projection onto  $\sum_n |\phi_n\rangle\langle\phi_n|$  in the spectral language), and  $\sigma_R^{\text{cont}}(\Delta E)$  is the non-resonant contribution to the same reaction cross section over the window (an  $R$ -matrix background-pole contribution to  $\sigma_R$ , a direct non-resonant capture amplitude, or a smooth absorptive optical-model continuum). By construction,  $\sigma_R$  is the reaction (non-elastic-breakup) cross section of Eq. (1); the elastic  $x+A$  scattering branch of  $\psi_x$ , which feeds the elastic-breakup amplitude at the three-body level (Sec. II), enters  $\sigma_{\text{elastic}}$  rather than  $\sigma_R$ .  $R$ -matrix hard-sphere phase shifts and the real elastic part of any smooth optical  $U_x$  therefore do not contribute to  $\sigma_R^{\text{cont}}$ . Within this restriction  $\sigma_R^{\text{res}}(\Delta E) + \sigma_R^{\text{cont}}(\Delta E) \simeq \sigma_R^{\text{tot}}(\Delta E)$  up to the (A2)-bounded pole-continuum interference. The smallness of  $\epsilon_{(A2)}$  must be assessed within the chosen continuum model rather than asserted from Coulomb penetration alone, since the entrance-channel penetrability is common to both  $\sigma_R^{\text{res}}$  and  $\sigma_R^{\text{cont}}$  and cancels in the ratio; the physical source of  $\epsilon_{(A2)} \ll 1$  at sub-Coulomb energies in light-nuclei reactions of astrophysical interest is the sparse level density and the dominance of isolated narrow resonances within the energy windows around the anchor pole. Explicit closure at a specific benchmark resonance through a chosen continuum model ( $R$ -matrix background-pole fit to  $\sigma_R$  or smooth absorptive optical-model continuum) is deferred to the companion application paper. (A2) is therefore a model-dependent diagnostic rather than a tabulation-only closed bound like (A1) and (A3).

The validity of (A3) is the requirement that the resonance half-width is small against the spacing to the nearest neighbor of any spin and parity, which is necessary for each resonance to be resolvable as a separate pole of the spectral sum rather than overlapping with its neighbors. The complementary dense-resonance regime, in which  $\xi_n^{\text{IAV}} \gtrsim |E_n - E_m|$  and the diagonal ansatz no longer applies, is outside the scope of the present work and is discussed only as outlook in Sec. VI.

When the three conditions (A1), (A2), (A3) hold

to a controlled accuracy, the diagonal action of  $W_x$  on the pole basis  $\{|\phi_n\rangle\}$  converts the matrix element  $\langle\psi_x(\mathbf{k}_b)|W_x|\psi_x(\mathbf{k}_b)\rangle$  in Eq. (1) into the spectral sum (2) with the Lorentzian profile (3). Conditions (A1) and (A3) admit explicit dimensionless analytical bounds in terms of the partial widths and level spacings of the participant-target subsystem [Eqs. (6)–(7) for (A1), and the half-width-to-spacing ratio for (A3)]; condition (A2) admits a model-dependent dimensionless diagnostic  $\epsilon_{(A2)}$  [Eq. (8)] on a specified continuum model. The smallness of  $\epsilon_{(A2)}$  at sub-Coulomb energies reflects the sparse participant-target level density within the energy window of interest, and must be verified case-by-case at the anchor resonance through the chosen continuum model. The spectral form (2) is therefore a narrow-resonance approximation under two closed dimensionless bounds and one model-dependent diagnostic: (A1) and (A3) close from  $R$ -matrix tabulations alone as  $\Gamma/D \rightarrow 0$ , while (A2) is assessed once a continuum model is specified, with the model dependence absorbed into the systematic uncertainty of the ansatz. The narrow-resonance limit of the spectral form (2), in which  $\omega_n$  collapses to a Dirac delta on the resonance energy, recovers the THM extraction and is the focus of the present analysis (Sec. VI); the overlapping-resonance regime, in which the diagonal ansatz no longer applies and the spectral sum would reorganize under additional averaging assumptions, is discussed there only as outlook.

For light-nuclei narrow-resonance reactions of astrophysical interest, comprehensive  $R$ -matrix evaluations [2, 5, 20] supply the tabulated partial widths and level energies that feed the bounds for (A1) and (A3), and place the controlling ratios at small dimensionless values at sub-Coulomb energies; the model-dependent  $\epsilon_{(A2)}$  closes once a specific  $R$ -matrix background-pole fit or smooth absorptive optical-model continuum is fixed at the anchor resonance, and the explicit verification at the resonances of any specific reaction belongs to the application paper that targets that reaction.

#### IV. WIDTH DICTIONARY, INTEGRATED-POLE-AREA, AND CHANNEL PROJECTION

The literature on indirect methods for narrow-resonance extraction suffers from three recurring ambiguities: between the half-width  $\Gamma/2$  and the full width  $\Gamma$  at half maximum, between sign conventions for the imaginary part of the optical potential, and between the spectral pole half-width  $\xi_n^{\text{IAV}}$  defined through Eqs. (2)–(3) and the experimental partial decay widths  $\Gamma_x^n$  and  $\Gamma_c^n$  that govern the branching of the resonance into its participant-channel and non-elastic decay channels respectively. I make the dictionary explicit before deriving any quantitative result.

The convention adopted throughout this manuscript is that the imaginary part of the absorptive optical poten-

tial is non-positive,  $W_x \leq 0$ , so that the operator  $-W_x$  is positive semidefinite and absorbs flux from the elastic channel. The diagonal matrix element  $\langle\phi_n|W_x|\phi_n\rangle \equiv W_n$  is therefore non-positive, and I define the spectral pole half-width-at-half-maximum (HWHM) as the positive quantity  $\xi_n^{\text{IAV}} \equiv |W_n| = -W_n > 0$ . The full-width-at-half-maximum (FWHM) participant-channel and non-elastic-channel partial widths  $\Gamma_x^n, \Gamma_c^n$  and the total width  $\Gamma_n^{\text{tot}}$  follow the uppercase  $\Gamma$  convention throughout. The original derivation of Ref. [32] kept the negative sign and worked with  $W_n$  directly; the dictionary between the two conventions is the single substitution  $W_n = -\xi_n^{\text{IAV}}$ , with no change of physical content. In the narrow-resonance limit, the spectral pole half-width is one half the non-elastic partial-width sum, which coincides with one half the experimental total decay width at sub-Coulomb energies where  $\Gamma_x^n \ll \Gamma_n^{\text{non-el}}$ ,

$$\xi_n^{\text{IAV}} = \frac{1}{2} \Gamma_n^{\text{non-el}} \simeq \frac{1}{2} \Gamma_n^{\text{tot}} = \frac{1}{2} \left( \Gamma_x^n + \sum_{c \neq x} \Gamma_c^n \right), \quad (9)$$

in which  $\Gamma_n^{\text{tot}} = \sum_c \Gamma_c^n$  is the experimental total decay width of the resonance  $n$  summed over all open decay channels (the participant channel and the non-elastic decay channels; for the  $^{19}\text{F} + p$  application of immediate interest in this work,  $x = p$  and the non-elastic channels are  $\alpha$  and  $\gamma$ ), and the approximate-equality sign in the first identity collapses to a strict equality whenever the participant-channel partial width  $\Gamma_x^n$  is negligible against the non-elastic decay width, with the residual relative correction controlled by the dimensionless ratio  $\Gamma_x^n/\Gamma_n^{\text{tot}}$  that is Coulomb-suppressed at sub-Coulomb energies for charged  $x$ . Equation (9) is established by a three-layer Feshbach decomposition that separates three physically distinct roles. The loose phrasing “ $W_x$  absorbs into all open channels” conflates them, and the conflation is the source of the recurring ambiguity in the literature between  $\xi_n^{\text{IAV}}$  on the one hand and  $\Gamma_x^n$  on the other [3, 32]. The three layers are:

- (A) **Layer A: pole self-energy of the IAV Green function on  $W_x$ .** The diagonal action of  $W_x$  on  $\phi_n$  generates the imaginary pole displacement of the IAV Green function  $G_x = (E_x - T_x - U_x)^{-1}$  with complex  $U_x$ , which fixes the half-width of the inclusive Lorentzian as  $\xi_n^{\text{IAV}} = |\langle\phi_n|W_x|\phi_n\rangle|$ .
- (B) **Layer B: channel projection of  $W_x$  on the non-elastic decay manifold.** The same diagonal matrix element is identified, through the Lane-Thomas  $R$ -matrix level-matrix imaginary part, with the sum of non-elastic partial widths,  $|\langle\phi_n|W_x|\phi_n\rangle| = \Gamma_n^{\text{non-el}}/2$ .
- (C) **Layer C: formation amplitude through the participant-channel entrance reduced width.** The per-pole DWBA pole amplitude of Eq. (4) inherits the overall normalization of  $\phi_n$ , which is set by the entrance reduced width  $\gamma_x^2$  and connects

to the participant-channel partial width  $\Gamma_x^n$  in the single-particle limit.

Each layer is established in turn below.

*Layer A: pole self-energy of the IAV Green function on the absorptive operator  $W_x$ .* The participant-spectator wavefunction  $\psi_x$  of Eq. (1) is the solution of an inhomogeneous Schrödinger equation with complex  $U_x$  and outgoing-wave boundary conditions, with the source set by the post-form interaction [27, 31, 32]. The IAV Green function  $G_x(E_x) = (E_x - T_x - U_x)^{-1}$  that resolves  $\psi_x$  on the pole basis is therefore a retarded complex- $U_x$  propagator, not a projection of  $G_x$  onto a subspace orthogonal to the elastic  $x + A$  channel. The pole self-energy  $\Sigma_n^{\text{IAV}}(E)$  on the bare resonance form factor  $\phi_n$  has its real part absorbed into the experimental pole position  $E_n$  by the construction of  $\phi_n$  as the interior eigenfunction of  $T_x + V_x^R$  at eigenvalue  $E_n$  (in the  $R$ -matrix convention of Sec. II), and has its imaginary part generated entirely by the diagonal action of  $W_x$  on  $\phi_n$ . Within the diagonal isolated-pole ansatz (5),  $G_x$  near the pole at  $E_x = E_n$  takes the form

$$G_x(E_x) \simeq \frac{|\phi_n\rangle\langle\phi_n|}{E_x - E_n + i\xi_n^{\text{IAV}}}, \quad (10)$$

in which the imaginary pole displacement is set by  $-\text{Im}\Sigma_n^{\text{IAV}} = \xi_n^{\text{IAV}} = |\langle\phi_n|W_x|\phi_n\rangle|$  and the resonance pole sits at  $E_x = E_n - i\xi_n^{\text{IAV}}$  in the lower complex half-plane (retarded convention). The Lorentzian intensity peak observed in the inclusive yield of Eq. (1) therefore has full width at half maximum  $2\xi_n^{\text{IAV}}$ , set by the diagonal matrix element of  $W_x$  on the pole; the elastic-channel content of  $\psi_x$  does not contribute to the imaginary pole displacement on  $\phi_n$  because  $\text{Im}\Sigma_n^{\text{IAV}}$  is generated by  $W_x$  alone; the corresponding elastic-breakup amplitude contributes separately to the elastic-breakup cross section rather than to the inclusive non-elastic-breakup yield of Eq. (1). In practice,  $\xi_n^{\text{IAV}}$  is not evaluated as a direct radial integral on  $W_x(r)$  (which would require a smooth-on-the-resonance-scale profile that the sub-Coulomb regime explicitly lacks, Sec. V) but is read from the experimentally tabulated partial widths through the Lane-Thomas identification of Layer B below [Eq. (11)], combined with the sub-Coulomb approximation  $\Gamma_n^{\text{non-el}} \simeq \Gamma_n^{\text{tot}}$  of Eq. (9); Layer A serves as the conceptual anchor that fixes the physical meaning of  $\xi_n^{\text{IAV}}$ , and Layer B supplies the operational shortcut.

*Layer B: channel projection of the absorptive operator  $W_x$  as a working identification.* The absorptive operator  $W_x$  represents flux removal from the elastic  $x + A$  channel into its complement, that is, into the open non-elastic channels  $c \neq x$ . The standard Lane-Thomas  $R$ -matrix construction [3, 42] identifies the imaginary part of the participant-target level matrix on the pole  $\lambda$  (the absorption of flux into open decay channels) with the channel sum  $\sum_c P_c \gamma_{\lambda c}^2 = \frac{1}{2} \sum_c \Gamma_\lambda^c$ , in which  $\Gamma_\lambda^c \equiv 2P_c \gamma_{\lambda c}^2$  are the FWHM partial widths built from the reduced widths  $\gamma_{\lambda c}^2$  and the channel penetration factors  $P_c$ . In the IAV

setting where  $W_x$  encodes the flux removed from the elastic channel into the non-elastic decay manifold (with the elastic-channel content of  $\psi_x$  carried by its outgoing-wave asymptotic amplitude and not entering the matrix element of Eq. (1)), the corresponding identification at the diagonal pole matrix element is

$$|\langle\phi_n|W_x|\phi_n\rangle| = \frac{1}{2} \sum_{c \neq x} \Gamma_c^n = \frac{1}{2} \Gamma_n^{\text{non-el}}, \quad (11)$$

in which  $\Gamma_n^{\text{non-el}} = \sum_{c \neq x} \Gamma_c^n$  (for the  $^{19}\text{F} + p$  resonances of immediate interest,  $x = p$  and  $\Gamma_n^{\text{non-el}} = \Gamma_\alpha^n + \Gamma_\gamma^n$ ). The restriction  $c \neq x$  in Eq. (11) is the IAV convention's specialization of the standard Lane-Thomas channel sum (which runs over all open channels including elastic participant re-emission): the IAV inclusive non-elastic-breakup yield of Eq. (1) is by construction restricted to absorption out of the elastic channel, with the elastic-breakup amplitude carried separately by the asymptotic outgoing-wave structure of  $\psi_x$  as documented in Layer A above. The partial widths  $\Gamma_c^n$  on the right-hand side are the experimentally measured (or  $R$ -matrix-fitted) decay-channel widths of the resonance  $n$ , and the equality is the spectral-ansatz statement that the diagonal absorptive matrix element on the pole form factor matches the corresponding sum-of-partial-widths reading of the Lane-Thomas level-matrix imaginary part. Layers A and B therefore both give  $\xi_n^{\text{IAV}} = \Gamma_n^{\text{non-el}}/2$  from the same operator  $W_x$ : Layer A through the imaginary pole displacement of the IAV Green function, Layer B through the identification of the diagonal absorptive matrix element with the Lane-Thomas sum of non-elastic partial widths.

*Sub-Coulomb identification with the experimental total width.* The experimentally measured resonance width is the total decay width  $\Gamma_n^{\text{tot}} = \Gamma_x^n + \Gamma_n^{\text{non-el}}$ , in which  $\Gamma_x^n$  is the participant-channel partial width from elastic re-emission. The IAV-internal width  $\xi_n^{\text{IAV}} = \Gamma_n^{\text{non-el}}/2$  of Layers A and B coincides with  $\Gamma_n^{\text{tot}}/2$  whenever  $\Gamma_x^n \ll \Gamma_n^{\text{non-el}}$ , which is the generic case at sub-Coulomb energies for charged participants because  $\Gamma_x^n$  is suppressed by the participant-channel Coulomb penetration factor  $\sim \exp(-2\pi\eta_{xA})$  at large Sommerfeld parameter  $\eta_{xA} \gg 1$ . The identification (9) is therefore the strict equality  $\xi_n^{\text{IAV}} = \Gamma_n^{\text{non-el}}/2$  supplemented by the sub-Coulomb approximation  $\Gamma_n^{\text{non-el}} \simeq \Gamma_n^{\text{tot}}$  that is controlled by the dimensionless ratio  $\Gamma_x^n/\Gamma_n^{\text{tot}}$ .

Specializing to the  $^{19}\text{F} + p$  application of immediate interest (so that  $x = p$  and  $\Gamma_x^n \equiv \Gamma_p$ ), at the 11 keV  $1^+$  resonance the proton partial width  $\Gamma_p \approx 1.1 \times 10^{-28}$  eV [20] and the dominant  $\alpha_2$  partial width  $|\Gamma_{\alpha_2}| \approx 590$  eV [24], together with the upper bound  $\Gamma_{\gamma_1} < 5$  eV [24] on the  $\gamma$  channel, give a total decay width  $\Gamma_n^{\text{tot}} \simeq |\Gamma_{\alpha_2}| \sim 6 \times 10^2$  eV and a ratio  $\Gamma_p/\Gamma_n^{\text{tot}} \approx 2 \times 10^{-31}$ , so the sub-Coulomb identification holds with negligible relative correction. For the higher-lying anchors used in the literature two-anchor THM normalization the proton-channel Coulomb suppression is weaker, with  $\Gamma_p/\Gamma_n^{\text{tot}} \approx 1.6\%$  at the 323 keV

$1^+$  anchor [11, 20] and of the same order of magnitude at the 828 keV anchor by Coulomb-penetration scaling at fixed channel radius (explicit  $\Gamma_p$  tabulation at the 828 keV anchor is deferred to the companion application paper), and the identification holds at the percent level rather than to negligible relative precision. The residual percent-level elastic-channel correction at the higher anchors enters the present work through the systematic uncertainty budget of the operational comparison. It is, however, of the same order of magnitude as the partial-wave-coherence and post-form-remnant residuals that the per-pole DWBA pole amplitude carries (Layer C of the present decomposition and the post-form remnant decomposition of Sec. V); in any quantitative comparison of the IAV-DWBA-derived resonance strength with the literature factorized-PWIA-THM extraction at higher anchors, this percent-level structural systematic must be propagated alongside the structural correction and not dropped a priori as Coulomb-suppressed.

The signed convention  $W_n = -\xi_n^{\text{IAV}}$  recovers the original  $W_x \leq 0$  convention of Ref. [32] through the substitution  $\xi_n^{\text{IAV}} = -W_n$ , with no change of physical content. Layer C, the formation amplitude that controls how strongly the per-pole DWBA cross section couples to the participant entrance channel through the entrance reduced width  $\gamma_x^2$  of the resonance state  $\phi_n$ , is established next as a separate identification distinct from Layers A and B.

*Layer C: formation amplitude through the entrance reduced width.* The per-pole DWBA pole amplitude of Eq. (4) is linear in the overall normalization of the resonance form factor  $\phi_n$ , and is therefore controlled by the participant-channel entrance reduced width  $\gamma_x^2$ , not by the diagonal absorptive matrix element of  $W_x$  on the same pole. This is the third distinct width that enters the formalism. The single-particle limit makes the connection to  $\Gamma_x^n$  explicit. When the resonance  $n$  is dominated by a single participant-channel single-particle configuration with spectroscopic factor  $C^2S = 1$  and the form factor  $\phi_n$  is the interior eigenfunction of the real participant-target potential at the experimental resonance energy  $E_n$  (in the  $R$ -matrix convention of Sec. II), the surface amplitude  $u_l(a)$  of  $\phi_n$  at the participant-channel radius is fixed by the standard  $R$ -matrix sum-rule reduced-width construction

$$\Gamma_x^{\text{sp}} = 2 P_l(E_n, a) \gamma_x^2, \quad \gamma_x^2 = \frac{\hbar^2}{2\mu_{xA} a} |u_l(a)|^2, \quad (12)$$

with  $P_l(E_n, a)$  the standard  $R$ -matrix penetration factor at orbital angular momentum  $l$ ,  $a$  the participant-channel radius,  $\mu_{xA}$  the participant-target reduced mass, and  $u_l(r) = r \phi_n(r)$  the radial single-particle wavefunction normalized to unit probability over the interior region  $r \leq a$  in the standard  $R$ -matrix convention [3, 42]. In the single-particle limit, the unit-probability normalization of  $u_l$  on the interior fixes both the surface amplitude  $|u_l(a)|$  (and hence  $\gamma_x^2$ ) and the overall normalization of  $\phi_n$  entering Eq. (4). The per-pole DWBA pole

cross section therefore scales with  $\gamma_x^2$ , modulo a structural prefactor set by the matching of  $\chi_a^{(+)}, \chi_b^{(-)}$  to  $\phi_n$  in the matrix-element integrand; through Eq. (12) at fixed  $E_n$  this same scaling translates into a proportionality to the participant-channel partial width  $\Gamma_x^n$ . The scaling controlling the formation amplitude is therefore  $\Gamma_x^n$ , not the spectral pole half-width  $\xi_n^{\text{IAV}}$ :  $\Gamma_x^n$  is an asymptotic decay-channel observable that controls how strongly the formation amplitude couples to the participant entrance channel, while  $\xi_n^{\text{IAV}}$  is the imaginary pole displacement that controls the Lorentzian shape of the inclusive yield in  $E_x$ . Conflating the two would double-count, since  $\xi_n^{\text{IAV}}$  already aggregates the non-elastic decay channels through Eq. (11) and is identified with  $\Gamma_n^{\text{tot}}/2$  via Eq. (9) in the sub-Coulomb regime where  $\Gamma_x^n \ll \Gamma_n^{\text{non-el}}$ . The single-particle proportionality  $|\mathcal{M}_n^{\text{DWBA}}|^2 \propto \gamma_x^2$  is a limit, not a general identity. Outside the single-particle limit the resonance form factor  $\phi_n$  contains coherent partial-wave admixture, and the per-pole DWBA pole amplitude retains coherent angular-momentum information that the entrance reduced width  $\gamma_x^2$  alone does not encode; the angular-momentum-basis treatment of the IAV transfer matrix element that exposes this content explicitly was developed in Ref. [33]. This residual partial-wave content of Layer C, which the standard factorized PWIA-THM reduction discards by factorizing the projectile spectator-momentum distribution out and setting the binary subreaction vertex on shell at the resonance energy as enumerated in Sec. V, is the dynamical content carried by the per-pole DWBA pole amplitude of Eq. (4). The branching ratio  $b_c^n$  from the exclusive channel-projection construction (defined formally in Eq. (14) below) and the Lorentzian denominator of Layer A are common to both reductions and cancel in the operational comparison; the per-pole DWBA cross section relative to its PWIA-THM reduction differs only through the partial-wave coherence carried by Layer C and through the post-form remnant of  $V_{\text{post}}$  retained. The widths  $\xi_n^{\text{IAV}}, \Gamma_x^n, \Gamma_c^n, \Gamma_n^{\text{tot}}$  (summarized in Table I) are physically distinct and enter the formalism at the three different layers identified above.

The Lorentzian profile (3) has integrated unit area over the full real-energy axis,

$$\int_{-\infty}^{+\infty} dE_x \omega_n(E_x) = 1, \quad (13)$$

which expresses the unit normalization of the Lorentzian. The product  $\omega_n(E_n) \cdot 2\xi_n^{\text{IAV}}$  at the peak therefore equals  $2/\pi$  regardless of the half-width, and the integrated-pole-area formulation (13) of the spectral form makes the resonance-strength extraction independent of the half-width versus full-width convention. The full-axis integral of Eq. (13) is the idealized statement; in any actual measurement the spectator-momentum gate, threshold cuts, and finite detector resolution restrict the integration to a finite window and convolve the integrand with an instrumental response, the modeling of which is an experimental-side modification outside the scope of the

TABLE I. The widths entering the Breit-Wigner spectral form of the IAV inclusive non-elastic breakup cross section, the channel projection, and the per-pole DWBA pole amplitude. Conventions and entry points are referenced to the equation labels of the text.

| symbol  | convention  | where it enters  |
|---|---|--|
| $\xi_n^{\text{IAV}} =  \langle \phi_n   W_x   \phi_n \rangle $    | half-width (HWHM) of the spectral Lorentzian; positive  | Lorentzian denominator of $\omega_n$ , Eq. (3); related to $\Gamma_n^{\text{tot}}$ by Eq. (9)  |
| $\Gamma_n^{\text{tot}} = \Gamma_x^n + \sum_{c \neq x} \Gamma_c^n$ | full width (FWHM) summed over the participant channel and all open non-elastic decay channels; positive   | total decay width of the resonance $n$ ; identified strictly with $2\xi_n^{\text{IAV}} = \Gamma_n^{\text{non-el}}$ via Layer B of the width dictionary [Eq. (9)], with the approximation $\Gamma_n^{\text{non-el}} \simeq \Gamma_n^{\text{tot}}$ controlled at sub-Coulomb energies by $\Gamma_x^n \ll \Gamma_n^{\text{non-el}}$ |
| $\Gamma_x^n$  | partial decay width of the participant entrance channel; positive ( $\Gamma_x^n \equiv \Gamma_p$ for the $^{19}\text{F} + p$ application of immediate interest) | strength of $ \mathcal{M}_n^{\text{DWBA}} ^2$ , Eq. (4), in the single-particle limit, Eq. (12)  |
| $\Gamma_c^n$ ( $c \neq x$ )                                       | partial decay widths of the non-elastic decay channels; positive ( $\Gamma_\alpha^n$ and $\Gamma_\gamma^n$ for the $^{19}\text{F} + p$ application)             | decay branching $b_c^n = \Gamma_c^n / \Gamma_n^{\text{tot}}$ in the channel projection   |

present work and is treated case-by-case in the THM literature [3, 17]. I use the integrated-pole-area property in particular when projecting the inclusive cross section on a single decay channel below.

The experimental observable in a typical resonant THM application is the exclusive channel-gated yield associated with a specific decay channel  $c$  of the participant-target subsystem. The projection from the inclusive non-elastic breakup of Eq. (2) onto this exclusive channel follows the usual formation-decay separation of an isolated resonance, and is best stated as a three-step factorization that keeps the role of each width in the dictionary of Sec. IV explicit. The per-pole formation cross section integrated over the resonance pole area is the product of the per-pole DWBA pole cross section of Eq. (4) and the integrated-pole-area unit normalization of the Lorentzian profile (3); call this object  $\sigma_n^{\text{form}}$ . The IAV inclusive non-elastic breakup yield  $\sigma_n^{\text{NEB}}$  accounts for the fraction of the formed resonance that decays into a non-elastic channel rather than re-emitting through the participant entrance channel, and is therefore  $\sigma_n^{\text{NEB}} = (\Gamma_n^{\text{non-el}} / \Gamma_n^{\text{tot}}) \sigma_n^{\text{form}}$ . The exclusive yield in a specific non-elastic channel  $c$  then selects  $c$  out of the non-elastic decay manifold with branching weight  $\Gamma_c^n / \Gamma_n^{\text{non-el}}$ , and the chain composes to

$$\sigma_n^{\text{excl},c} = \frac{\Gamma_c^n}{\Gamma_n^{\text{non-el}}} \sigma_n^{\text{NEB}} = \frac{\Gamma_c^n}{\Gamma_n^{\text{tot}}} \sigma_n^{\text{form}} \equiv b_c^n \sigma_n^{\text{form}}, \quad (14)$$

with the standard formation-decay branching ratio  $b_c^n = \Gamma_c^n / \Gamma_n^{\text{tot}}$  defined relative to the experimental total width. In the sub-Coulomb regime where  $\Gamma_n^{\text{non-el}} \simeq \Gamma_n^{\text{tot}}$ , the intermediate factor  $\Gamma_n^{\text{non-el}} / \Gamma_n^{\text{tot}}$  collapses to unity and  $\sigma_n^{\text{form}} \simeq \sigma_n^{\text{NEB}}$ , so that the experimentally familiar form  $\sigma_n^{\text{excl},c} \simeq b_c^n \sigma_n^{\text{NEB}}$  is recovered. The factorization (14) is in the integrated-pole-area sense of Eq. (13), and rests on the formation-decay separation that the formation amplitude of  $\phi_n$  in the IAV mechanism is set by the transfer

matrix element of Eq. (4) and the decay branching is a structure property of the resonance independent of the formation mechanism. The cancellation of  $b_c^n$  between the IAV-DWBA-derived and the literature PWIA-THM-derived exclusive extractions follows because the branching ratio is identical in the per-pole DWBA pole amplitude and in its non-perturbative reduction to the factorized PWIA-THM expression of the same parent inclusive cross section. The cancellation is exact within the scalar isolated-pole branching approximation; corrections enter through the off-diagonal absorptive couplings  $W_{nm}$  and through level interference, and are estimated to be of the same order as the Cauchy-Schwarz bound (6) on  $W_{nm}$  in terms of the partial widths and level spacings of the relevant participant-target subsystem. The projection (14) is the analytical statement that the operational extraction comparison developed below applies to the exclusive observable through the same cancellation that holds at the inclusive level.

## V. CONTROLLED POST-FORM SOURCE AT SUB-COULOMB ENERGIES

The transfer matrix element of Eq. (4) is the post-form expression of the resonance pole amplitude and is the starting point of the second reduction in Fig. 1, which lists the four steps that take the per-pole DWBA pole amplitude to the factorized PWIA-THM expression. The post-form interaction is

$$V_{\text{post}} = V_{bx} + (U_{bA} - U_{bB}), \quad (15)$$

in which  $V_{bx}$  is the spectator-participant interaction binding the projectile  $a = b + x$ ,  $U_{bA}$  is the spectator-target optical potential, and  $U_{bB}$  is the spectator-residual optical potential. The first term  $V_{bx}$  is the direct breakup interaction; the second term, the difference  $U_{bA} - U_{bB}$ , is

the post-form remnant that arises because the spectator-target distortion in the entrance arrangement differs from the spectator-residual distortion in the exit arrangement.

The choice of the post-form expression as the central source convention of this manuscript is dictated by a physical obstacle specific to the sub-Coulomb astrophysical regime, not by a stylistic preference. The corresponding prior-form transition operator is  $V_{\text{prior}} = V_x^R + (U_{bA} - U_{aA})$ , where  $V_x^R$  is the same real participant-target interaction generating the resonance form factor in the  $R$ -matrix interior convention of Sec. II,  $(T_x + V_x^R)\phi_n = E_n\phi_n$ , and  $U_{aA}$  is the entrance projectile-target optical potential. In the sub-Coulomb regime the absorptive part  $W_x = \text{Im}U_x$  is not smooth on the resonance scale: it is dominated by sparse narrow resonances rather than by a smooth megaelectronvolt-scale optical envelope. The standard global nucleon optical-model parametrizations of Ref. [43], with nominal validity from 1 keV to 200 MeV, fit their lowest-energy depth parameters to *average resonance parameters* of the participant-target subsystem and therefore average over precisely the narrow-resonance structure that the spectral ansatz (5) is built to resolve. By dispersion the real part  $\text{Re}U_x$  inherits the same sparse-pole structure from  $W_x$ , so the candidate identification  $V_x^R \equiv \text{Re}U_x$  cannot be controllably approximated by a smooth global Woods-Saxon parametrization in the sub-Coulomb regime. A controlled prior-form construction would therefore require either an explicit  $R$ -matrix expansion of the participant-target Green function over the pole basis  $\{\phi_n\}$  or a separate pole-by-pole assembly of  $V_x^R$ ; both are alternative formalisms with their own validity conditions and lie outside the scope of the present manuscript. The post-form transition operator (15), in contrast, contains no such  $V_x^R$  in the operator itself. The resonance structure still enters through  $\phi_n$ , but the operator acting between entrance and exit channels is fixed by projectile structure through  $V_{bx}$  and by spectator-channel optical potentials  $U_{bA}$  and  $U_{bB}$  at well-separated kinematics where smooth Woods-Saxon parametrizations are standard. I therefore adopt the post-form expression as the central convention throughout, with the prior-form construction acknowledged only as a separate formalism beyond the scope of the present analysis.

The first plane-wave limit of the transfer matrix element of Eq. (4) is obtained by replacing the entrance and exit distorted waves by plane waves,

$$\chi_a^{(+)}(\mathbf{k}_a, \mathbf{r}_a) \rightarrow e^{i\mathbf{k}_a \cdot \mathbf{r}_a}, \quad \chi_b^{(-)}(\mathbf{k}_b, \mathbf{r}_b) \rightarrow e^{-i\mathbf{k}_b \cdot \mathbf{r}_b}, \quad (16)$$

This single substitution defines a plane-wave Born transfer cross section,

$$\frac{d\sigma_n^{\text{PWBA}}}{d\Omega_b} = \frac{2\pi \rho_b}{\hbar v_a} \left| \langle \phi_n e^{-i\mathbf{k}_b \cdot \mathbf{r}_b} | V_{\text{post}} | e^{i\mathbf{k}_a \cdot \mathbf{r}_a} \phi_a \rangle \right|^2. \quad (17)$$

Equation (17) is not yet the factorized PWIA-THM expression used in resonance-strength extraction. The latter requires, in addition to the plane-wave substitution

that defined Eq. (17), three further reductions [steps (ii)–(iv) of the four-step chain enumerated below]: (ii) zero-range or finite-range surface-localized treatment of  $V_{bx}$ , in which the spectator-participant interaction inside the projectile is taken to act at the relative coordinate  $\mathbf{r}_{bx} = 0$  or with a short-range form factor, (iii) on-shell evaluation of the binary subreaction vertex at the kinematic point set by the spectator-window cuts, and (iv) restriction to the  $V_{bx}$  piece of  $V_{\text{post}}$ , with the remnant  $U_{bA} - U_{bB}$  dropped on the basis that it is suppressed at the surface-localized vertex. The combined reduction yields the standard factorized form

$$\frac{d\sigma_n^{\text{PWIA-THM}}}{d\Omega_b} = \mathcal{N}_{\text{kin}}(\Omega_b, k_b) |\tilde{\phi}_a(\mathbf{p}_{bx})|^2 \times |T_{xA \rightarrow n}^{\text{on}}(E_n; \mathbf{q})|^2, \quad (18)$$

in which  $\tilde{\phi}_a$  is the Fourier transform of the projectile internal wavefunction evaluated at the  $b$ - $x$  relative momentum  $\mathbf{p}_{bx}$ ,  $\mathbf{q} = \mathbf{k}_a - \mathbf{k}_b$  is the momentum transfer,  $T_{xA \rightarrow n}^{\text{on}}(E_n; \mathbf{q})$  is the on-shell binary  $T$ -matrix element for the resonant  $x + A \rightarrow n$  subreaction at participant-target relative momentum  $\mathbf{q}$  and pole energy  $E_n$ , in the operational form adopted by the literature PWIA-THM extraction protocol [3, 6, 11] (so that  $|T_{xA \rightarrow n}^{\text{on}}|^2$  at the resonance peak carries the formation-decay product  $\Gamma_x^n \Gamma_c^n / \Gamma_n^{\text{tot}}$  that defines the astrophysical resonance strength  $(\omega\gamma)_n^c$  of Eq. (24) below), and  $\mathcal{N}_{\text{kin}}$  collects the spectator-window phase-space, spin-average, and Jacobian factors common to the adopted THM convention. Equation (18) is the form that underlies the standard PWIA-THM extraction formula [6, 11]. The three further reductions (ii)–(iv), together with the plane-wave substitution (i), are made explicit so that the difference between the DWBA matrix element of Eq. (4) and Eq. (18) can be attributed to identifiable physical content rather than to an unspecified distortion correction.

In the THM literature, the combined four-step reduction of Eq. (18) is operationally tied to the quasi-free (QF) kinematic condition: spectator-detection cuts select configurations at the peak of the bound-state momentum amplitude  $|\tilde{\phi}_a(\mathbf{p}_{bx})|^2$ , which for the s-wave-dominated Trojan Horses in standard use lies at  $\mathbf{p}_{bx} \approx 0$ . The QF condition is itself a kinematic event-selection prescription rather than a dynamical approximation in Eq. (18); the plane-wave substitution of step (i) and the on-shell binary-vertex evaluation of step (iii) are independent dynamical approximations applied at the QF kinematic point, neither of which is implied by  $\mathbf{p}_{bx} \approx 0$  alone. The MDWBA framework of Ref. [17] retains entrance and exit distortions on the same QF kinematic selection without invoking step (i), and resonant HOES-THM expressions retain the off-shell binary vertex without invoking step (iii); the four-step reduction of the present analysis combines both. The per-pole DWBA pole amplitude of Eq. (4) is therefore not constrained to the QF kinematic point and can be evaluated at any spectator kinematics within the validity of the spectral ansatz, with

the proviso that quantitative THM extraction requires that the direct three-body transfer mechanism be empirically validated at the chosen kinematics.

The on-shell evaluation of the binary subreaction vertex in step (iii) of the four-step chain is the on-shell limit of the half-off-energy-shell (HOES) extrapolation that has been extensively treated in the THM literature. The earliest analytic HOES treatment of an elastic two-body subreaction in the THM context, restricted to s-wave separable Yamaguchi potentials, was given by Tumino, Mukhamedzhanov *et al.* [12]; the standard THM review of Ref. [3] reorganizes the off-shell-to-on-shell extrapolation through the binary-vertex form factor. The resonant-THM extension was developed by Mukhamedzhanov and collaborators through the generalized  $R$ -matrix and surface-integral framework [13–15, 44], with the resonant working formula collected in the recent THM review of Tumino *et al.* [17] as a sum of isolated non-interfering one-level / two-channel  $R$ -matrix HOES amplitudes. These resonant-HOES expressions retract the on-shell binary-vertex approximation but operate on the plane-wave reduction of the entrance and exit channels.

A separate line of work, the modified-DWBA (MD-WBA) framework of the same review of Ref. [17], retains full distorted waves on the entrance and exit channels but operates on the binary subreaction at an on-shell extraction stage; this framework retracts the plane-wave substitution but retains the on-shell binary-vertex evaluation. The per-pole DWBA pole amplitude of Eq. (4), embedded in the BW spectral form (2) of the inclusive non-elastic breakup parent, retracts both the plane-wave substitution and the on-shell binary-vertex evaluation simultaneously through the post-form transfer matrix element on the resonance state  $\phi_n$ , with the post-form remnant content of  $V_{\text{post}}$  retained. This combination of the BW spectral decomposition of the inclusive parent with full distorted waves and post-form remnant in the per-pole transfer amplitude has not appeared in the published THM literature.

The DWBA pole amplitude of Eq. (4) admits the operator-side decomposition

$$|\mathcal{M}_n^{\text{DWBA}}|^2 = |T_n^{\text{direct}}|^2 + |T_n^{\text{remnant}}|^2 + 2 \text{Re}(T_n^{\text{direct}} * T_n^{\text{remnant}}), \quad (19)$$

in which

$$T_n^{\text{direct}} = \langle \phi_n \chi_b^{(-)} | V_{bx} | \chi_a^{(+)} \phi_a \rangle, \quad (20)$$

$$T_n^{\text{remnant}} = \langle \phi_n \chi_b^{(-)} | U_{bA} - U_{bB} | \chi_a^{(+)} \phi_a \rangle. \quad (21)$$

Equations (17) and (18) together expose the standard factorized PWIA-THM working formula of Refs. [6, 11] as a *non-perturbative reduction* of the per-pole DWBA pole amplitude of Eq. (4) under four identifiable approximations: (i) the plane-wave substitution (16), (ii) the zero-range or surface-localized treatment of  $V_{bx}$ , (iii) the on-shell binary-vertex evaluation  $T_{xA \rightarrow n}^{\text{on}}(E_n; \mathbf{q})$ , and (iv)

the post-form remnant neglect that drops  $T_n^{\text{remnant}}$  in favor of  $T_n^{\text{direct}}$  alone. The four approximations do not constitute a perturbative limit with a small parameter that interpolates continuously between Eq. (4) and Eq. (18); they are, rather, finite reductions, each of which removes a specific dynamical content of the per-pole transfer matrix element. The four steps are sequentially identifiable as discrete reductions at this scale; this is distinct from the finer-scale statement below that step (i) itself decomposes into three physics layers (Coulomb wavefunction, nuclear phase shift on the surface, and interior amplitude) that are not separately switchable within step (i). The present analysis therefore does not introduce a multiplicative dynamical correction factor on top of Eq. (18); the operational quantity for sub-Coulomb resonance-strength extraction is the per-pole DWBA pole cross section  $d\sigma_n^{\text{DWBA}}/d\Omega_b$  of Eq. (4) itself, with the partial-wave coherence within  $T_n^{\text{direct}}$  and the post-form remnant content of  $T_n^{\text{remnant}}$  retained.

The intermediate plane-wave Born object of Eq. (17) appears only as an intermediate stage in the four-step reduction; it is not a privileged “reference state” against which the per-pole DWBA pole cross section of Eq. (4) could be expressed as a multiplicative correction factor in the sub-Coulomb regime of the binary subreaction. The reason is structural: at sub-Coulomb binary relative energies the binary Sommerfeld parameter  $\eta_{xA} \gg 1$  governs the small-radius behavior of  $\phi_n$  non-perturbatively, since the Born series in the binary Coulomb interaction has zero radius of convergence at the origin in the  $\eta_{xA} \rightarrow \infty$  limit. The plane-wave Born substitution (16) separately removes three layers of physics from the entrance and exit distorted waves  $\chi_a^{(+)}, \chi_b^{(-)}$  (Coulomb wavefunction, nuclear phase shift in the  $S$ -matrix on the surface, and interior amplitude inside the nuclear surface), all of which derive from the same coupled radial Schrödinger equation with the same complex optical potential. When integrated against the non-perturbative  $\phi_n$  in the matrix element of Eq. (4), these three layers do not admit independently switchable corrections through a graded perturbative ordering, because their effects on the small-radius matching of  $\chi_a^{(+)}, \chi_b^{(-)}$  with  $\phi_n$  are convolved with the Coulomb-modified short-range structure of  $\phi_n$  itself, even when the projectile-target and spectator-residual Sommerfeld parameters  $\eta_{aA}, \eta_{bB}$  are moderate at the THM kinematics. There is therefore no convergent perturbative ordering by which the DWBA pole amplitude can be reconstructed from the plane-wave Born amplitude through a controlled sequence of corrections at sub-Coulomb energies of the binary subreaction. At binary energies above the Coulomb barrier the small-radius structure of  $\phi_n$  is smooth on the relevant length scale and the analogous ordering of the three layers against  $\phi_n$  is well-defined in principle; the present manuscript is restricted to the sub-Coulomb regime where it is not.

Empirical evidence from a quantitative study of ( $d, pX$ ) inclusive non-elastic breakup [45] provides an above-barrier baseline that documents one part of the

structural argument independently. Even the much milder radial cut-off prescription, which retains the full  $S$ -matrix  $S_l = e^{2i(\sigma_l + \delta_l^{\text{nucl}})}$  on the asymptotic surface form  $u_l(r) \rightarrow (i/2)[H_l^{(-)}(r) - S_l H_l^{(+)}(r)]$  and zeroes only the interior region  $r < R_{\text{cut}}$ , deviates from the full IAV result by 20–25% in deuteron-induced reactions at incident energies well above the Coulomb barrier, with the deviation localized in the interior of the wavefunction and growing with incident energy. This datum demonstrates that the interior amplitude of the entrance and exit distorted waves carries non-negligible dynamical content already in a regime where Coulomb suppression is absent. The plane-wave Born substitution strips, in addition to this interior amplitude, two further layers: the nuclear phase shift on the surface and the Coulomb wavefunction outside the nuclear surface. The role of Ref. [45] in the present argument is therefore supporting rather than extrapolative: it documents the necessity of the interior amplitude in a regime where the Coulomb amplification is absent, while the sub-Coulomb conclusion that the plane-wave Born expression cannot serve as a reference state is established independently in the next paragraph through the structure-dependent matching of the entrance and exit distorted waves with the resonance form factor  $\phi_n$ , which the plane-wave substitution disrupts non-perturbatively at sub-Coulomb energies of the binary subreaction.

Within Eqs. (4) and (17) the resonance form factor  $\phi_n$  is identical, and the binary-subreaction Sommerfeld parameter  $\eta_{xA} \gg 1$  that characterizes the sub-Coulomb astrophysical regime enters the matrix element only through  $\phi_n$ , common to both expressions; the absolute ratio  $\sigma_n^{\text{DWBA}}/\sigma_n^{\text{PWBA}}$  is therefore not dominated by a multiplicative Gamow factor on  $\phi_n$ . The Gamow penetration factor  $\sim \exp(-2\pi\eta_{xA})$  does enter the further-reduced PWIA-THM expression of Eq. (18) explicitly through the on-shell binary cross section  $|T_{xA \rightarrow n}^{\text{on}}(E_n; \mathbf{q})|^2$ , and is computable there through the standard  $R$ -matrix penetrability  $P_l(E_n, a)$  of Refs. [3, 44]; this factor is universal and structure-independent in the sense that it depends only on the binary entrance-channel charges, the relative energy, and the channel radius, not on the dynamical content of the per-pole transfer amplitude. The structure-dependent residue between Eq. (4) and Eq. (17) that would be of physical interest as a “correction” is set instead by the matching of  $\chi_a^{(+)}$ ,  $\chi_b^{(-)}$  to  $\phi_n$  in the matrix-element integrand, and does not factor out as a controlled multiplicative correction since the three layers of physics described above are not independently switchable, even when the projectile-target and spectator-residual Sommerfeld parameters  $\eta_{aA}$ ,  $\eta_{bB}$  are moderate by the THM choice that places the projectile-target system above its Coulomb barrier. Eq. (17) therefore cannot serve as the diagnostic baseline for an entrance- and exit-distortion correction at sub-Coulomb energies. The operational quantity is the per-pole DWBA pole cross section of Eq. (4) itself, with the partial-wave coherence and post-form remnant

content of the parent transfer matrix element retained.

The cancellation of the branching ratio  $b_c^n$ , established in Sec. IV, ensures that the per-pole DWBA pole cross section  $d\sigma_n^{\text{DWBA}}/d\Omega_b$  multiplies the inclusive and exclusive yields by the same channel factor within the scalar isolated-pole branching approximation, so the same factor multiplies the corresponding non-perturbative reduction of  $d\sigma_n^{\text{DWBA}}/d\Omega_b$  to Eq. (18). Any operational comparison of the IAV-DWBA-derived exclusive yield to the literature PWIA-THM-derived exclusive yield is therefore independent of  $b_c^n$  to leading order in the ansatz.

## VI. ISOLATED-RESONANCE LIMIT AND OUTLOOK ON THE OVERLAPPING-RESONANCE REGIME

The Lorentzian spectral form (2)-(3) admits two regime limits that are distinguished by the ratio  $\xi_n^{\text{IAV}}/|E_n - E_m|$  of the resonance half-width to the nearest-neighbor level spacing. The isolated-resonance limit,  $\xi_n^{\text{IAV}} \ll |E_n - E_m|$ , is the regime relevant to sub-Coulomb THM extraction and is the focus of this section; the overlapping-resonance regime,  $\xi_n^{\text{IAV}} \gtrsim |E_n - E_m|$ , lies outside the scope of the diagonal isolated-pole ansatz and is discussed at the end of the section as outlook.

The isolated-resonance limit is defined by  $\xi_n^{\text{IAV}} \ll |E_n - E_m|$  for the nearest neighbor of any spin and parity. In this limit the Lorentzian profile (3) collapses to a Dirac delta on the resonance energy in the distributional sense, since the unit-area Lorentzian of half-width  $\xi_n^{\text{IAV}}$  converges weakly to  $\delta(E_x - E_n)$  as  $\xi_n^{\text{IAV}} \rightarrow 0$  when integrated against any test function smooth on the level-spacing scale,

$$\omega_n(E_x) \xrightarrow{\xi_n^{\text{IAV}} \rightarrow 0} \delta(E_x - E_n). \quad (22)$$

Operationally, when integrated against any test function  $F(E_x)$  smooth on the level-spacing scale and over a window  $\Delta E$  obeying  $\xi_n^{\text{IAV}} \ll \Delta E \ll |E_n - E_m|$ , the spectral weight acts as  $\int_{\Delta E} dE_x \omega_n(E_x) F(E_x) \simeq F(E_n)$  to leading order in  $\xi_n^{\text{IAV}}/|E_n - E_m|$  and in the bin-width-to-spacing ratio. The spectral sum (2) then becomes a sum over single-pole transfer matrix elements evaluated at  $E_x = E_n$ .

Combining the isolated-resonance limit (22) and the channel-projection (14), the per-pole exclusive spectator yield in the spectator window takes the form

$$\frac{d^2 \sigma_n^{\text{excl},c}}{d\Omega_b dE_b} = b_c^n \frac{d\sigma_n^{\text{DWBA}}}{d\Omega_b} \delta(E_x - E_n), \quad (23)$$

in which  $d\sigma_n^{\text{DWBA}}/d\Omega_b$  of Eq. (4) is the per-pole DWBA pole cross section evaluated on the resonance state  $\phi_n$  with full entrance and exit distortions and the post-form interaction  $V_{\text{post}}$ , and the branching ratio  $b_c^n$  projects the inclusive yield onto the experimentally gated decay channel  $c$ . Equation (23) is the analytical statement that

the IAV inclusive non-elastic breakup parent reduces, in the isolated-resonance limit and within the diagonal isolated-pole ansatz, to a per-pole DWBA pole cross section weighted by the channel branching ratio. It is the zero-detector-resolution idealization; the finite quasi-free spectator acceptance and detector response of an actual THM measurement convolve the integrand with the experimental window, as already noted after Eq. (13) in Sec. IV. The standard factorized PWIA-THM working formula of Refs. [6, 11] is the non-perturbative reduction of  $d\sigma_n^{\text{DWBA}}/d\Omega_b$  under the four approximations identified at Eq. (18) (plane-wave substitution, zero-range or surface-localized  $V_{bx}$ , on-shell binary vertex, and post-form remnant neglect); replacing the per-pole DWBA pole cross section in Eq. (23) by Eq. (18) recovers the factorized literature working form. The validity of (A3) and of the Cauchy-Schwarz bound on (A1), together with the continuum-decoupling diagnostic of (A2) on the leakage of  $W_x$  into the genuine  $x+A$  continuum at the anchor resonance, controls how accurately the delta collapse (22) holds at a given resonance, while the framework retains, through the partial-wave coherence of the per-pole matrix element of Eq. (4) and through the post-form remnant decomposition of Sec. V, the dynamical content of the transfer matrix element that the plane-wave reduction (16) and the further three approximations (ii)–(iv) of Sec. V suppress.

*Operational extraction recipe.* Equation (23) sets the computational workflow for extracting a sub-Coulomb THM resonance strength within the present framework. The inputs at the anchor resonance  $n$  are: the level energy  $E_n$ , the participant-channel partial width  $\Gamma_x^n$ , and the non-elastic-channel partial widths  $\{\Gamma_c^n\}_{c \neq x}$  from  $R$ -matrix tabulations (for the  $^{19}\text{F} + p$  application of immediate interest,  $\Gamma_x^n = \Gamma_p$  and  $\{\Gamma_c^n\} = \{\Gamma_\alpha^n, \Gamma_\gamma^n\}$ ); a real participant-target potential  $V_x^R$  tuned so that the interior eigenvalue equals  $E_n$ , fixing the interior form factor  $\phi_n$  on  $r \leq a$  in the  $R$ -matrix convention of Sec. II (the asymptotic Coulomb tail is not constructed explicitly but is encoded through the surface amplitude  $u_l(a)$  and the tabulated partial widths); the entrance and exit optical potentials  $U_{aA}$  and  $U_{bB}$  generating the distorted waves  $\chi_a^{(+)}$ ,  $\chi_b^{(-)}$ ; the spectator-target optical potential  $U_{bA}$  entering the post-form remnant of  $V_{\text{post}}$ ; the projectile internal wavefunction  $\phi_a$ ; and the spectator-participant binding interaction  $V_{bx}$ . For first-pass comparison with the literature factorized-PWIA-THM extraction the spectroscopic factor of  $\phi_n$  in the participant-channel configuration is set to  $C^2S = 1$ , matching the single-particle convention of Refs. [6, 11]; relaxation of this convention multiplies  $|\mathcal{M}_n^{\text{DWBA}}|^2$  by the corresponding  $C^2S$  and belongs to a structure-corrected analysis.

The per-pole DWBA matrix element of Eq. (4) is evaluated by standard finite-range DWBA quadrature on the real radial axis. The interior support of  $\phi_n$  on  $r_x \leq a$  bounds the bra-side integration, and the bound-state  $\phi_a$  provides the asymptotic damping in the spectator coordinate, so the post-form transfer integrand

is well-behaved and standard transfer codes apply directly. Contour deformation techniques such as Vincent-Fortune complex-contour integration [46, 47], which are required for the unprojected inclusive IAV expectation value on the outgoing-wave participant-spectator wavefunction  $\psi_x$ , are not needed for the per-pole DWBA on the  $R$ -matrix interior form factor  $\phi_n$  adopted in the present framework. Any residual Coulomb-remnant tail of  $U_{bA} - U_{bB}$  at large spectator-target separation has a point-Coulomb piece  $\sim -Z_b Z_x e^2/R$  that vanishes identically when the projectile decomposition  $a = b + x$  satisfies  $Z_b Z_x = 0$ ; this includes the deuteron-induced Trojan Horses (where either  $b$  or  $x$  is the neutron) employed in the benchmark applications of Refs. [6, 11], so that only the short-range nuclear difference of  $U_{bA} - U_{bB}$  remains in the integrand. For projectiles where  $Z_b Z_x \neq 0$ , the standard remedies of screened Coulomb potentials or Vincent-Fortune complex-contour integration in the spectator coordinate [46, 47] restore absolute convergence; their numerical implementation belongs to the companion application paper. The bound-state projectile wavefunction  $\phi_a$  in the integrand additionally provides exponential damping in the spectator-participant relative coordinate, bounding the matrix element on the real radial axis once the spectator-target Coulomb behavior has been handled.

Multiplying  $d\sigma_n^{\text{DWBA}}/d\Omega_b$  by the branching ratio  $b_c^n = \Gamma_c/\Gamma_n^{\text{tot}}$  and integrating over the spectator-window kinematics returns the channel-gated yield to be compared with the THM measurement. The astrophysical resonance strength of the decay channel  $c$  is defined, following the conventions of Refs. [2, 3, 5], as

$$(\omega\gamma)_n^c \equiv \frac{2J_n + 1}{(2j_x + 1)(2j_A + 1)} \frac{\Gamma_x^n \Gamma_c^n}{\Gamma_n^{\text{tot}}}, \quad (24)$$

with  $J_n$  the resonance spin and  $j_x, j_A$  the participant and target ground-state spins; the compound symbol  $\omega\gamma$  is the standard astrophysical resonance-strength notation and is not a product of the spectral Lorentzian profile  $\omega_n(E_x)$  of Eq. (3) with a width  $\gamma$ . The recipe is applied in two operational modes that should be kept distinct. In the *forward-consistency mode*, all partial widths on the right-hand side of Eq. (24) are taken as fixed inputs from  $R$ -matrix tabulations or higher-energy direct measurements, and the predicted IAV-DWBA yield is compared with the measured THM yield as a consistency check on the per-pole DWBA framework itself. In the *extraction mode*, one partial width at the sub-Coulomb target anchor (typically the  $\alpha$ - or  $\gamma$ -decay width that is inaccessible to direct measurement at sub-Coulomb energies) is treated as a free fit parameter, with the absolute normalization and the remaining widths fixed at higher-energy anchor resonances where they are independently constrained from direct measurement; the two-anchor weighted-average normalization protocol of Ref. [11] is one realization of this mode. The IAV-DWBA extraction  $(\omega\gamma)_n^{\text{DWBA}}$  obtained from  $b_c^n d\sigma_n^{\text{DWBA}}/d\Omega_b$  replaces the factorized PWIA-THM working extraction

$(\omega\gamma)_n^{\text{PWIA-THM}}$  of Refs. [6, 11] at the decay channel  $c$  of physical interest; the structural difference between the two extractions is the dynamical content carried by the four-step reduction of Sec. V (entrance-exit distortions, finite-range  $V_{bx}$ , off-shell binary vertex, post-form remnant), to be evaluated case by case at the benchmark of interest. Absolute comparison to the measured triple-differential yield requires that the spectator-window cuts, decay-angle gating, efficiency, and energy-resolution folding of the experimental analysis be applied to the calculated integrand, in the same conventions used by the THM measurement.

The complementary regime  $\xi_n^{\text{IAV}} \gtrsim |E_n - E_m|$  across the energy window of interest is relevant to compound-nucleus reactions at intermediate and high energies. In this regime the diagonal isolated-pole ansatz (5) is no longer a controlled approximation: the off-diagonal elements  $W_{nm}$  no longer satisfy a small-ratio bound and the spectral sum (2) cannot be evaluated pole by pole. A reorganization of the spectral sum into a smooth absorptive potential and the corresponding Hauser-Feshbach surrogate-method form [41, 48] would require three additional conditions: energy averaging of the inclusive cross section over a window  $\Delta E$  obeying the dense-regime hierarchy  $D \lesssim \xi_n^{\text{IAV}} \ll \Delta E \ll \Delta E_{\text{phys}}$ , where  $D$  is the local mean level spacing and  $\Delta E_{\text{phys}}$  is the energy scale on which physical observables vary; random relative phases of the off-diagonal couplings  $W_{nm}$  across the averaging window; and the local-density approximation that replaces the discrete sum of pole strengths by a smooth integral over a local level density. The second condition is the random-phase assumption underlying the compound-nucleus picture of Bohr. A quantitative analysis of these conditions on a high-level-density benchmark, and the corresponding connection to the IAV-revival numerical literature [37–39, 41] that targets compound-nucleus indirect inference, is left to future work; the present analysis is restricted to the isolated-resonance regime relevant to sub-Coulomb THM extraction.

## VII. CONNECTION TO EXISTING LITERATURE

The position of the present framework relative to the existing analytical and numerical literature on indirect resonance-strength extraction can be summarized along five axes: the spectral structure of the participant-target absorptive potential, the entrance and exit distorted waves on the three-body process, the binary subreaction vertex evaluation, the post-form remnant content, and the application scope. The diagonal isolated-pole spectral representation of  $W_x$  in Eq. (5) is the ingredient that distinguishes the present analysis from the smooth-optical assumption used in the IAV-revival [37–39] and Lei-Moro 2018 [32] numerical lines; the entrance and exit distorted waves are retained on the three-body process in the same spirit as the modified-DWBA discussion of

Ref. [17]; the binary subreaction vertex is implicit in the per-pole DWBA matrix element of Eq. (4) without an additional half-off-shell extrapolation step; and the post-form remnant is retained through the decomposition of Eq. (19). The application scope is the sub-Coulomb resonant THM regime, in which the spectral ansatz (5) and the post-form decomposition (19) jointly enable an analytical link between the parent inclusive cross section and the per-resonance THM extraction.

Three differentiations from the prior literature are worth singling out. (i) Ref. [36] retains the half-off-shell binary vertex and the Coulomb Jost / vertex form factor in its analytical framework but evaluates only a renormalization factor in the production calculation, built from the ratio of zero-range DWBA cross sections weighted by the spectator momentum distribution, in which the off-shell function, the Coulomb Jost function, and the vertex form factor cancel or are absent. Their conclusion that the inclusion of distorted waves eliminates a sharp rise of the indirect  $S$ -factor at sub-Coulomb energies is therefore a phenomenological Coulomb-distortion correction obtained from this spectator-weighted zero-range cross-section ratio, not a numerical evaluation of the full surface-integral expression. (ii) The Tumino *et al.* review [17] treats the resonant case as a sum of isolated non-interfering one-level two-channel  $R$ -matrix half-off-shell amplitudes; the closing paragraph of that resonant-case discussion itself invokes inclusive non-elastic-breakup theory [16] as exemplifying the two-step framework that would address the propagation of the transferred particle absent from the factorized form, and the IAV closed inclusive expression is later presented in a separate section of the same review, but the BW spectral projection of Ref. [32] that links the parent inclusive cross section to a per-pole transfer matrix element is not constructed. The present framework supplies that analytical link by making the isolated-pole validity conditions (A1) and (A3) explicit through the dimensionless bounds of Eqs. (6)–(7), and retains the entrance and exit distortions on the three-body process and the post-form remnant of  $V_{\text{post}}$ ; the resonant working formula of Ref. [17] adopts the isolated-non-interfering-pole assumption implicitly and operates on the plane-wave reduction of the entrance and exit channels. (iii) The earliest controlled treatment of off-energy-shell corrections in the THM context, by Tumino, Mukhamedzhanov, and collaborators [12], was restricted to elastic two-body subreactions and to  $s$ -wave separable Yamaguchi potentials; the present framework covers the resonance-plus-transfer topology with complex participant-target optical potential and arbitrary partial waves contained in the single transfer matrix element of Eq. (4), and the two are not directly comparable as analytical results.

I have previously demonstrated, in a separate numerical line, the convergence of the post-form *inclusive* IAV expectation value  $\langle \psi_x | W_x | \psi_x \rangle$  on the outgoing-wave participant-spectator wavefunction  $\psi_x$  by Vincent-Fortune complex-contour and hybrid methods at inter-

mediate energies of 25 and 50 MeV [46, 47]. The per-pole DWBA matrix element of Eq. (4) of the present framework operates on the  $R$ -matrix interior form factor  $\phi_n$  rather than on  $\psi_x$ , so the bra-side  $r_x$  integration is bounded by the channel radius and standard finite-range DWBA quadrature on the real radial axis is sufficient; the spectral projection eliminates the Coulomb-tail convergence problem that motivated the Vincent-Fortune treatment of the inclusive matrix element. Numerical verification of the per-pole DWBA at a specific resonant THM benchmark is left to the companion application paper.

A complementary numerical line by Liu, Lei, and Ren [45] examines the sensitivity of the IAV inclusive non-elastic breakup cross section to the interior part of the entrance and exit distorted waves through a radial cut-off scheme that retains the full asymptotic  $S$ -matrix on the surface and zeroes only the interior region. For deuteron-induced ( $d, pX$ ) reactions, the cut-off result is suppressed relative to the full IAV result by up to 20–25%, located in the interior of the wavefunction and growing with incident energy. This is the empirical input cited in Sec. V to support the structural reason why the plane-wave Born expression of Eq. (17) is retained only as an intermediate stage in the four-step non-perturbative reduction (18) and not as a privileged reference state.

## VIII. SUMMARY AND OUTLOOK

I have established three results for the IAV inclusive non-elastic breakup cross section in the sub-Coulomb resonant regime.

First, the diagonal isolated-pole spectral ansatz of the absorptive participant-target optical potential, Eq. (5), is controlled in the narrow-resonance regime under the dimensionless bounds of conditions (A1) and (A3) from  $R$ -matrix tabulations [Eqs. (6)–(7)] and the model-dependent diagnostic  $\epsilon_{(A2)}$  of Eq. (8) on the smooth  $x+A$  continuum.

Second, the width dictionary  $\xi_n^{\text{IAV}} = \Gamma_n^{\text{non-el}}/2 \simeq \Gamma_n^{\text{tot}}/2$ , derived through the three-layer Feshbach decomposition, separates the role of the absorptive operator  $W_x$  on the IAV Green function  $G_x = (E_x - T_x - U_x)^{-1}$  with complex  $U_x$ , the role of the channel projection that decomposes the non-elastic absorption into specific exit channels, and the role of the participant-channel entrance reduced width that controls the formation amplitude, and resolves the half-width-versus-full-width and sign-of-the-imaginary-potential ambiguities of the literature and the recurring conflation of the spectral pole half-width with the participant-channel partial width.

Third, the IAV inclusive non-elastic breakup cross section reduces in the isolated-resonance limit to a per-pole distorted-wave Born approximation transfer matrix element evaluated on the resonance state with full entrance and exit distortions and the post-form interaction, weighted by the channel branching ratio [Eq. (23)].

The post-form source is adopted as the central convention at sub-Coulomb energies because the prior-form alternative would require an explicit pole-by-pole assembly of  $V_x^R$  that is outside the scope of the present formalism (Sec. V).

The central operational statement of the manuscript follows from the three results above and is sharper than any of them individually. The factorized PWIA-THM resonance-strength expression of Refs. [6, 11] and the per-pole DWBA pole cross section of Eq. (4) are *successive reductions of the same IAV inclusive non-elastic breakup parent* (Fig. 1): the isolated-resonance limit of the diagonal spectral ansatz reduces the IAV inclusive parent to the per-pole DWBA pole cross section [Eq. (23)], and a four-step chain of Sec. V further reduces that per-pole DWBA pole cross section to the factorized PWIA-THM expression [Eq. (18)]. This further reduction is neither a perturbative expansion in a small parameter within the four-step chain, nor a multiplicative dynamical correction factor applied on top of the factorized form. The four approximations of the further reduction are: plane-wave substitution on the entrance and exit distorted waves, zero-range or surface-localized treatment of the spectator-participant interaction, on-shell evaluation of the binary subreaction vertex, and post-form remnant neglect. Within the diagonal isolated-pole ansatz, the operational quantity for sub-Coulomb resonance-strength extraction is therefore the per-pole DWBA pole cross section itself, with the partial-wave coherence within  $T_n^{\text{direct}}$  and the difference of optical potentials in  $T_n^{\text{remnant}}$  retained; these two pieces are the dynamical content of the per-pole transfer matrix element that the four-step reduction suppresses.

Operationally, the extraction is performed by computing  $b_c^n d\sigma_n^{\text{DWBA}}/d\Omega_b$  at the anchor resonance following the recipe given below Eq. (23), and the structural offset of the resulting  $(\omega\gamma)_n^{\text{DWBA}}$  from the literature factorized-PWIA-THM extraction  $(\omega\gamma)_n^{\text{PWIA-THM}}$  of Refs. [6, 11] is set by the four-step content of Sec. V and is evaluated case by case at the benchmark of interest.

*Calculation-level inputs versus concept-level diagnostic.* The numerical inputs of the recipe are the  $R$ -matrix reduced widths  $\gamma_x^2$  (participant channel) and  $\gamma_{\lambda_c}^2$  (non-elastic decay channels), related to the experimentally tabulated partial widths by  $\Gamma = 2P\gamma^2$ . The participant-channel reduced width  $\gamma_x^2$  fixes the surface amplitude of  $\phi_n$  and therefore the absolute scale of  $d\sigma_n^{\text{DWBA}}/d\Omega_b$  [Eq. (12)], while the non-elastic-channel reduced widths  $\gamma_{\lambda_c}^2$  supply the channel branching  $b_c^n = \Gamma_c^n/\Gamma_n^{\text{tot}}$ . The IAV spectral half-width  $\xi_n^{\text{IAV}}$ , by contrast, does not appear in the integrated-pole-area extraction formula (23); its role is to gate the diagonal isolated-pole ansatz through the dimensionless smallness parameters of validity conditions (A1) and (A3), and to set the Lorentzian half-width of the differential  $E_x$  shape. The three layers of the width dictionary (Sec. IV) are therefore separated also at the operational level:  $\gamma_x^2, \gamma_{\lambda_c}^2$  are calculation inputs at Layers C and B, while  $\xi_n^{\text{IAV}}$  at Layer A is a valid-

ity diagnostic that controls when the spectral framework applies but cancels in the integrated-pole-area limit of Eq. (13); a residual  $\xi_n^{\text{IAV}}$  dependence enters only when the experimental spectator window  $\Delta E$  is comparable to or narrower than  $\xi_n^{\text{IAV}}$ , an experimental-side modification treated case by case in the THM literature [3, 17].

The complementary overlapping-resonance regime of the same spectral form connects formally to the Hauser-Feshbach surrogate-method picture of compound-nucleus reactions under three additional averaging assumptions; a controlled derivation of that limit requires a separate

high-level-density benchmark and is left as outlook.

## ACKNOWLEDGMENTS

This work was supported by the National Natural Science Foundation of China (Grant Nos. 12475132 and 12535009) and the Fundamental Research Funds for the Central Universities. I acknowledge the use of large language model assistants for editorial polishing of the English text and for cross-validation of intermediate algebraic steps in the analytical derivations; all physics content, derivations, and conclusions are my own responsibility.

- 
- [1] G. Baur, *Phys. Lett. B* **178**, 135 (1986).  
 [2] C. Angulo *et al.*, *Nucl. Phys. A* **656**, 3 (1999).  
 [3] R. E. Tribble, C. A. Bertulani, M. La Cognata, A. M. Mukhamedzhanov, and C. Spitaleri, *Rept. Prog. Phys.* **77**, 106901 (2014).  
 [4] A. Tumino, C. A. Bertulani, M. La Cognata, L. Lamia, R. G. Pizzone, S. Romano, and S. Typel, *Ann. Rev. Nucl. Part. Sci.* **71**, 345 (2021).  
 [5] B. Acharya *et al.*, *Rev. Mod. Phys.* **97**, 035002 (2025).  
 [6] M. La Cognata *et al.*, *Astrophys. J.* **708**, 796 (2010).  
 [7] M. La Cognata, S. Palmerini, C. Spitaleri, I. Indelicato, A. M. Mukhamedzhanov, I. Lombardo, and O. Trippella, *Astrophys. J.* **805**, 128 (2015).  
 [8] I. Indelicato, M. La Cognata, C. Spitaleri, V. Burjan, S. Cherubini, M. Gulino, S. Hayakawa, Z. Hons, V. Kroha, L. Lamia, M. Mazzocco, J. Mrazek, R. G. Pizzone, S. Romano, E. Strano, D. Torresi, and A. Tumino, *Astrophys. J.* **845**, 19 (2017).  
 [9] G. L. Guardo, G. G. Rapisarda, D. L. Balabanski, *et al.*, *Universe* **10**, 304 (2024).  
 [10] T. Petruse, G. L. Guardo, D. Lattuada, M. La Cognata, D. L. Balabanski, *et al.*, *Eur. Phys. J. A* **61**, 4 (2025).  
 [11] X. D. Su, M. La Cognata, N. Vukman, *et al.*, *Phys. Rev. Lett.* **135**, 182701 (2025).  
 [12] A. Tumino, C. Spitaleri, A. Mukhamedzhanov, *et al.*, *Phys. Rev. C* **78**, 064001 (2008).  
 [13] A. M. Mukhamedzhanov and A. S. Kadyrov, *Phys. Rev. C* **82**, 051601 (2010).  
 [14] A. M. Mukhamedzhanov, *Phys. Rev. C* **84**, 044616 (2011).  
 [15] A. M. Mukhamedzhanov, A. S. Kadyrov, and D. Y. Pang, *Eur. Phys. J. A* **56**, 233 (2020).  
 [16] C. A. Bertulani, M. S. Hussein, and S. Typel, *Phys. Lett. B* **776**, 217 (2018).  
 [17] A. Tumino, C. A. Bertulani, S. Cherubini, *et al.*, *Prog. Part. Nucl. Phys.* **143**, 104164 (2025).  
 [18] I. Lombardo, D. Dell’Aquila, A. Di Leva, I. Indelicato, M. La Cognata, M. La Commara, A. Ordine, V. Rigato, M. Romoli, E. Rosato, G. Spadaccini, C. Spitaleri, A. Tumino, and M. Vigilante, *Phys. Lett. B* **748**, 178 (2015).  
 [19] L. Y. Zhang, A. Y. López, M. Lugaro, J. J. He, and A. I. Karakas, *Astrophys. J.* **913**, 51 (2021).  
 [20] R. J. deBoer, O. Clarkson, A. J. Couture, J. Görres, F. Herwig, I. Lombardo, P. Scholz, and M. Wiescher, *Phys. Rev. C* **103**, 055815 (2021).  
 [21] L. Redigolo, I. Lombardo, D. Dell’Aquila, A. Musumarra, M. G. Pellegriti, M. Russo, G. Verde, and M. Vigilante, *Nucl. Phys. A* **1060**, 123102 (2025).  
 [22] L. Y. Zhang and others (JUNA Collaboration), *Phys. Rev. Lett.* **127**, 152702 (2021).  
 [23] L. Y. Zhang and others (JUNA Collaboration), *Phys. Rev. C* **106**, 055803 (2022).  
 [24] L. Zhang, J. He, R. J. deBoer, M. Wiescher, A. Heger, *et al.*, *Nature* **610**, 656 (2022).  
 [25] Y.-J. Chen, H. Zhang, L.-Y. Zhang, J.-J. He, *et al.*, *Nucl. Sci. Tech.* **35**, 143 (2024).  
 [26] W. Liu, B. Guo, J. He, Z. Li, X. Tang, M. Lugaro, and G. Lian, *Ann. Rev. Nucl. Part. Sci.* **75**, 271 (2025).  
 [27] M. Ichimura, N. Austern, and C. M. Vincent, *Phys. Rev. C* **32**, 431 (1985).  
 [28] M. S. Hussein and K. W. McVoy, *Nucl. Phys. A* **445**, 124 (1985).  
 [29] N. Austern, Y. Iseri, M. Kamimura, M. Kawai, G. Rawitscher, and M. Yahiro, *Phys. Rept.* **154**, 125 (1987).  
 [30] J. Lei and A. M. Moro, *Phys. Rev. C* **92**, 044616 (2015), arXiv:1510.02602 [nucl-th].  
 [31] J. Lei and A. M. Moro, *Phys. Rev. C* **92**, 061602 (2015).  
 [32] J. Lei and A. M. Moro, *Phys. Rev. C* **97**, 011601 (2018).  
 [33] J. Lei, *Phys. Rev. C* **97**, 034628 (2018), arXiv:1712.01433 [nucl-th].  
 [34] J. Lei and A. M. Moro, *Phys. Rev. Lett.* **123**, 232501 (2019).  
 [35] J. Lei and A. M. Moro, *Phys. Rev. C* **108**, 034612 (2023), arXiv:2305.14111 [nucl-th].  
 [36] A. M. Mukhamedzhanov, D. Y. Pang, and A. S. Kadyrov, *Phys. Rev. C* **99**, 064618 (2019), arXiv:1806.08828 [nucl-th].  
 [37] G. Potel, F. M. Nunes, and I. J. Thompson, *Phys. Rev. C* **92**, 034611 (2015), arXiv:1508.04822 [nucl-th].  
 [38] B. V. Carlson, R. Capote, and M. Sin, *Few-Body Syst.* **57**, 307 (2016).  
 [39] G. Potel, G. Perdikakis, B. V. Carlson, *et al.*, *Eur. Phys. J. A* **53**, 178 (2017).  
 [40] B. V. Carlson, T. Frederico, and M. S. Hussein, *Phys. Lett. B* **767**, 53 (2017).  
 [41] J. E. Escher, J. T. Harke, F. S. Dietrich, N. D. Scielzo, I. J. Thompson, and W. Younes, *Rev. Mod. Phys.* **84**, 353 (2012).

- [42] A. M. Lane and R. G. Thomas, *Rev. Mod. Phys.* **30**, 257 (1958).
- [43] A. J. Koning and J. P. Delaroche, *Nucl. Phys. A* **713**, 231 (2003).
- [44] M. La Cognata, A. M. Mukhamedzhanov, C. Spitaleri, *et al.*, *Astrophys. J. Lett.* **739**, L54 (2011).
- [45] J. Liu, J. Lei, and Z. Ren, *Phys. Rev. C* **108**, 024606 (2023).
- [46] C. M. Vincent and H. T. Fortune, *Phys. Rev. C* **2**, 782 (1970).
- [47] J. Lei, *Phys. Rev. C* **112**, 014609 (2025), [arXiv:2504.03112](https://arxiv.org/abs/2504.03112) [nucl-th].
- [48] W. Hauser and H. Feshbach, *Phys. Rev.* **87**, 366 (1952).